Scope of the Lecture

1. Semiconductor lasers
2. DBR, DFB lasers
3. Vertical cavity lasers
4. Quantum cascade lasers
5. Lasers with rare-earth-doped dielectrics
6. Fiber lasers
7. Vibronic solid state lasers
8. Dye laser

Reading: Ch. 9

Homojunction

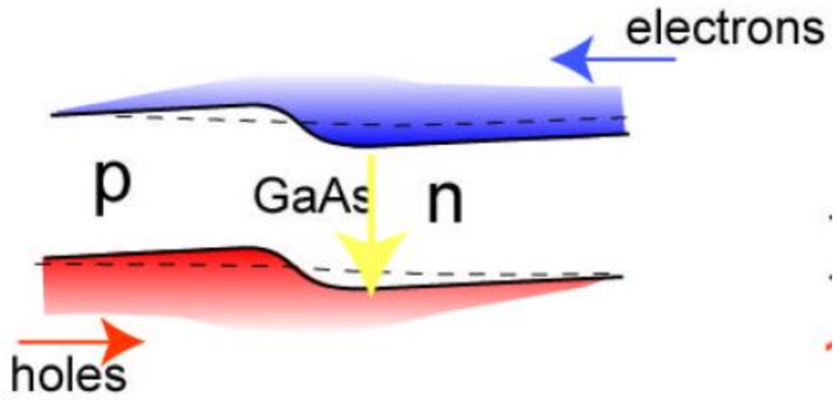

- no carrier confinement
- no optical waveguide

10kA/cm2 @ 10K

Heterojunction

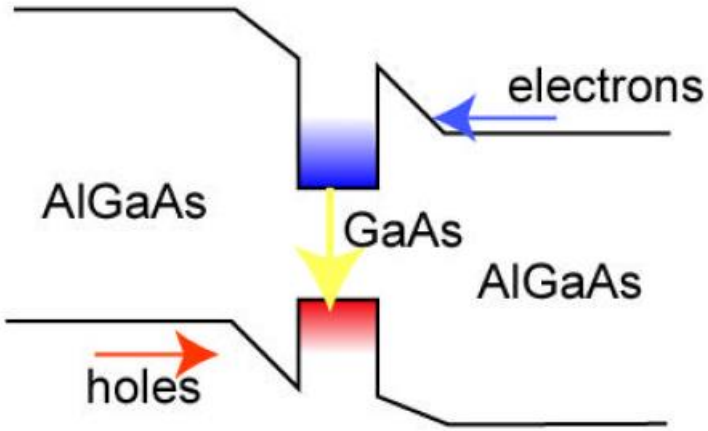

- electrons and holes confined
- optical waveguide

2kA/cm^2 @300K

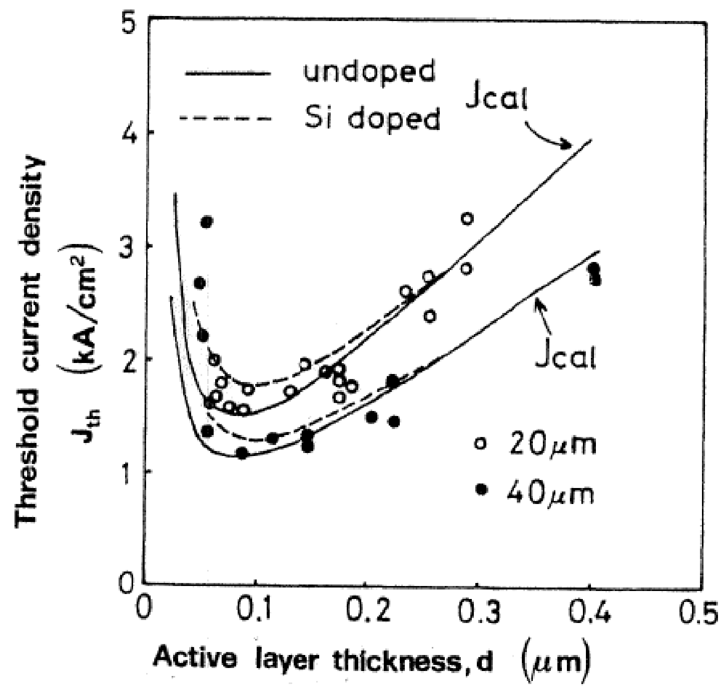

FIG. 9.23. Calculated (*continuous and dashed lines*) and experimental (*open and closed circles*) values of the threshold current density J_{th} versus active layer thickness d for a 300 μm long AlGaAs DH laser. Closed and open circles represent data for a 40-μm and 20-μm stripe width, respectively. Theoretical curves J_{cal} refer to cases of undoped and low Si-doped active layers. (By permission from Ref. 41.)

DH-LD

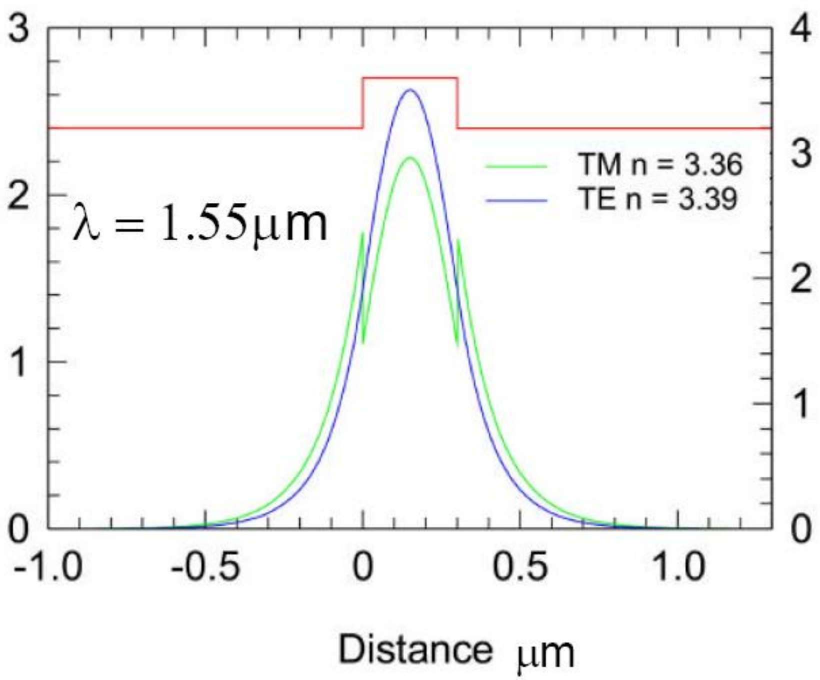

SCDHMQW-LD

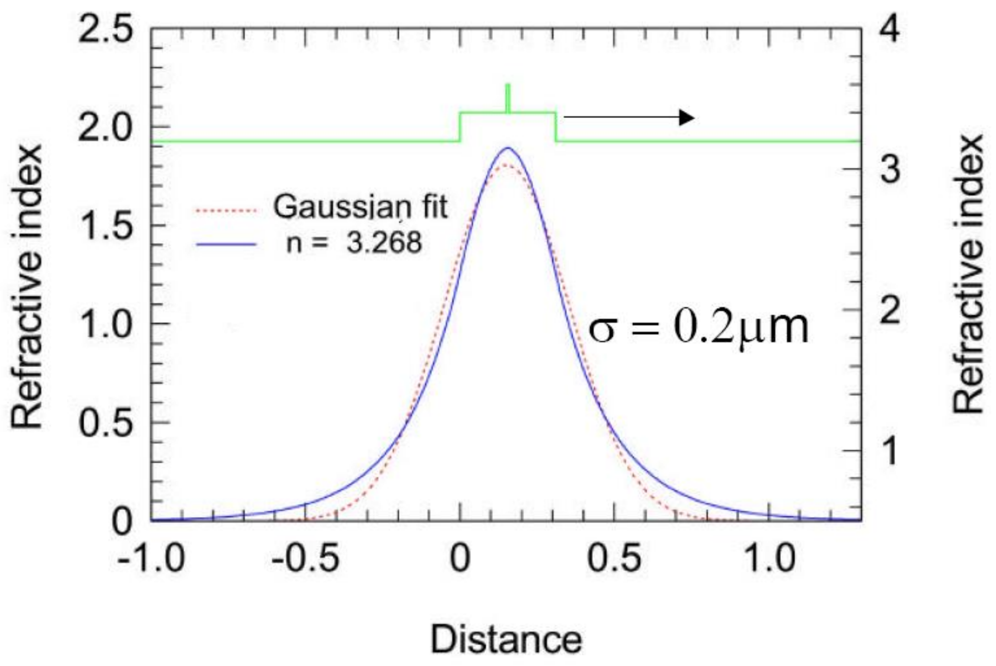

- TE mode better confined
- Lower laser threshold for TE

Output polarized in waveguide plane

- Separate confinement
- Reduce laser threshold

Fully engineerable structure

Semiconductor lasers

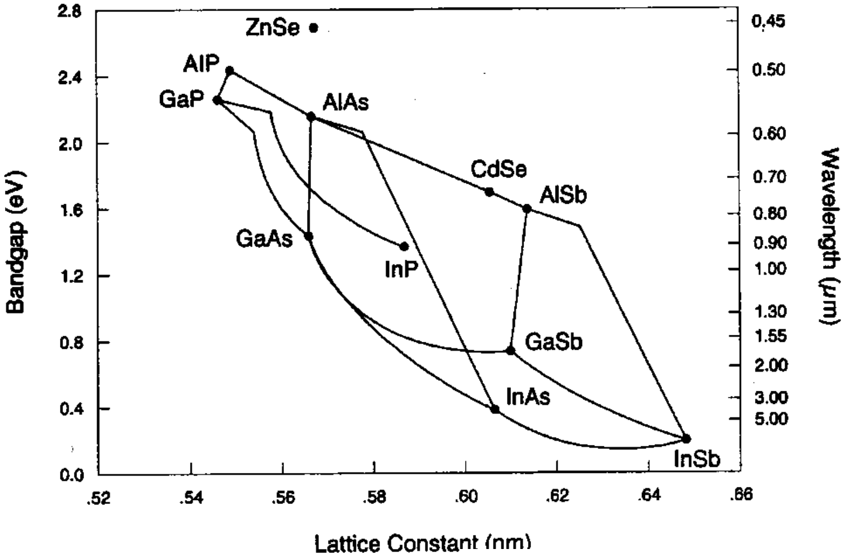

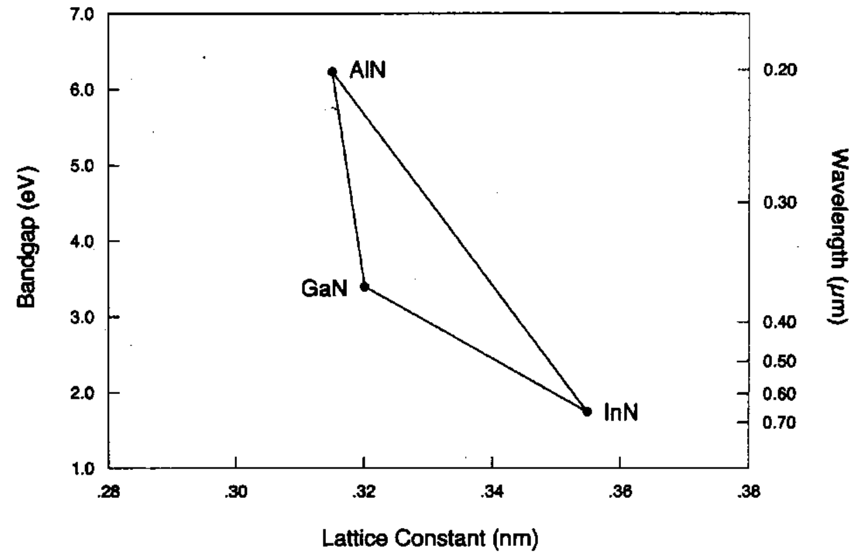

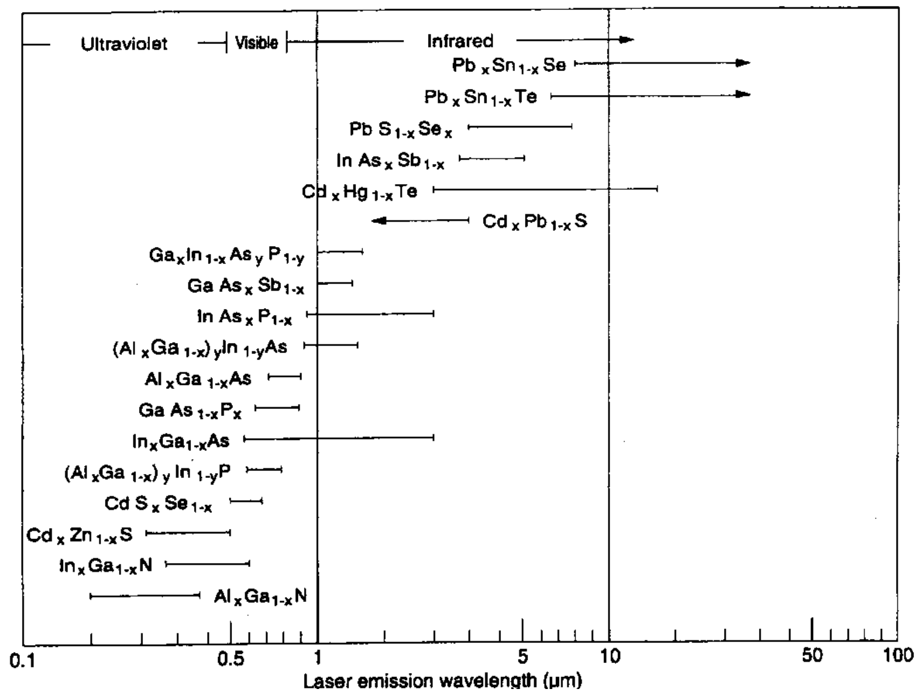

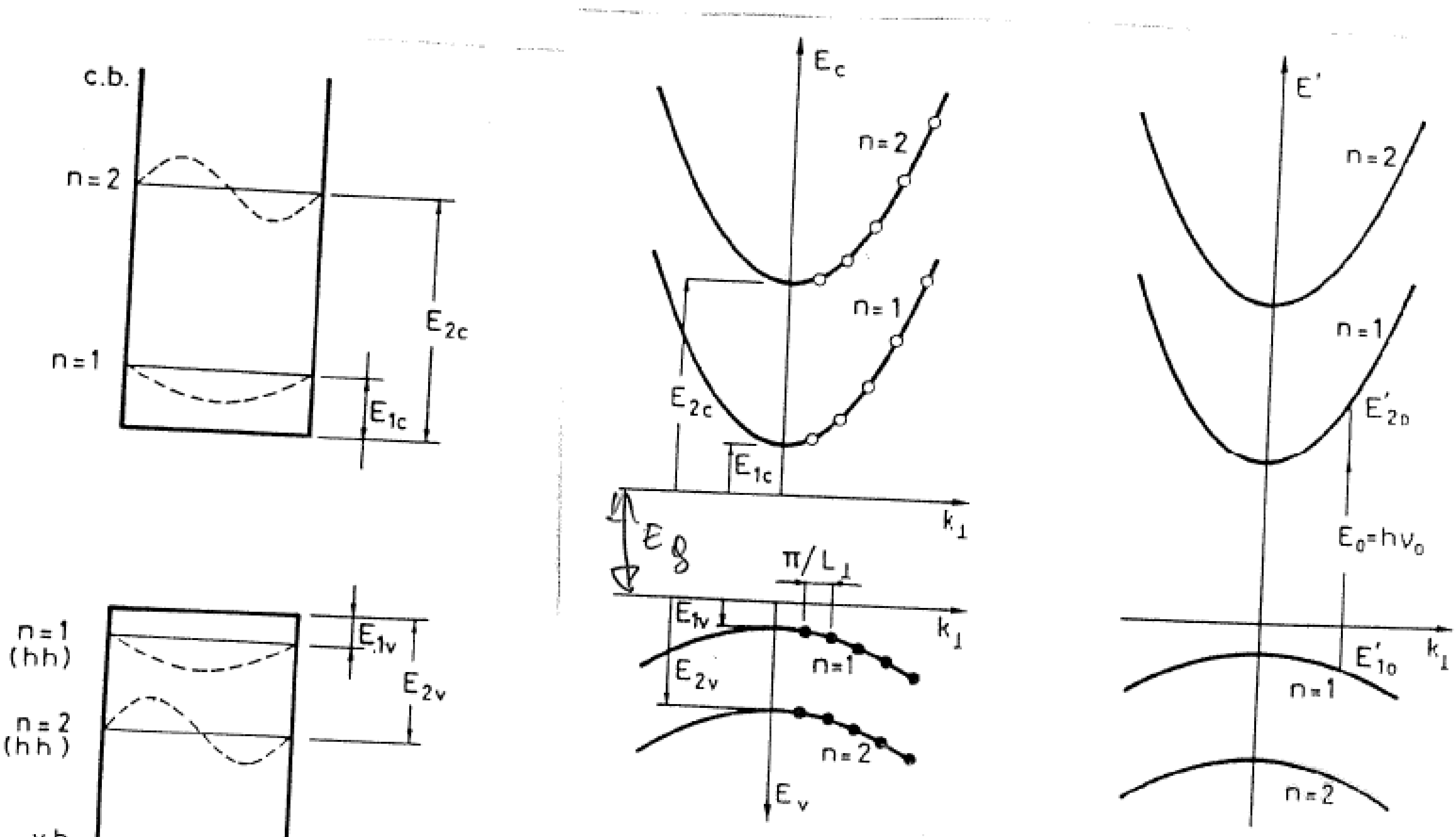
c.b.
n=2
n=1
E2c
E1c
n=1
(hh)
n=2
(hh)
E1v
E2v
v.b.
Ec
n=2
n=1
E2c
E1c
k⊥
Eg
π/L⊥
E1v
E2v
k⊥
n=1
n=2
Ev
E'
n=2
n=1
E'2o
E0=hν0
E'1o
k⊥
n=1
n=2

(a)

(b)

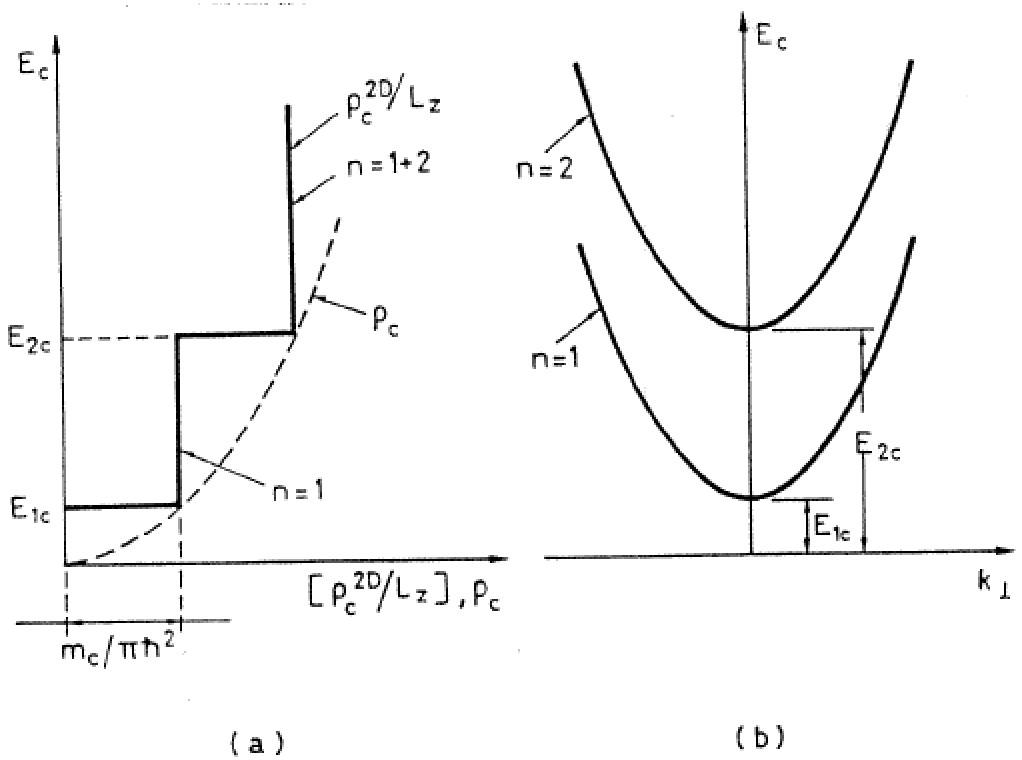

FIG. 3.25. (a) Plot of the quantum well density of states in the conduction band ρ_c^{2D} normalized to the well thickness L_z as a function of the state energy E_c (*staircase, solid line*). In the same figure, the plot of the density of states for the corresponding bulk semiconductor ρ_c is also shown as a dashed line. (b) Plots of the E_c versus $k_\perp$ relations for the $n=1$ and $n=2$ conduction subbands.

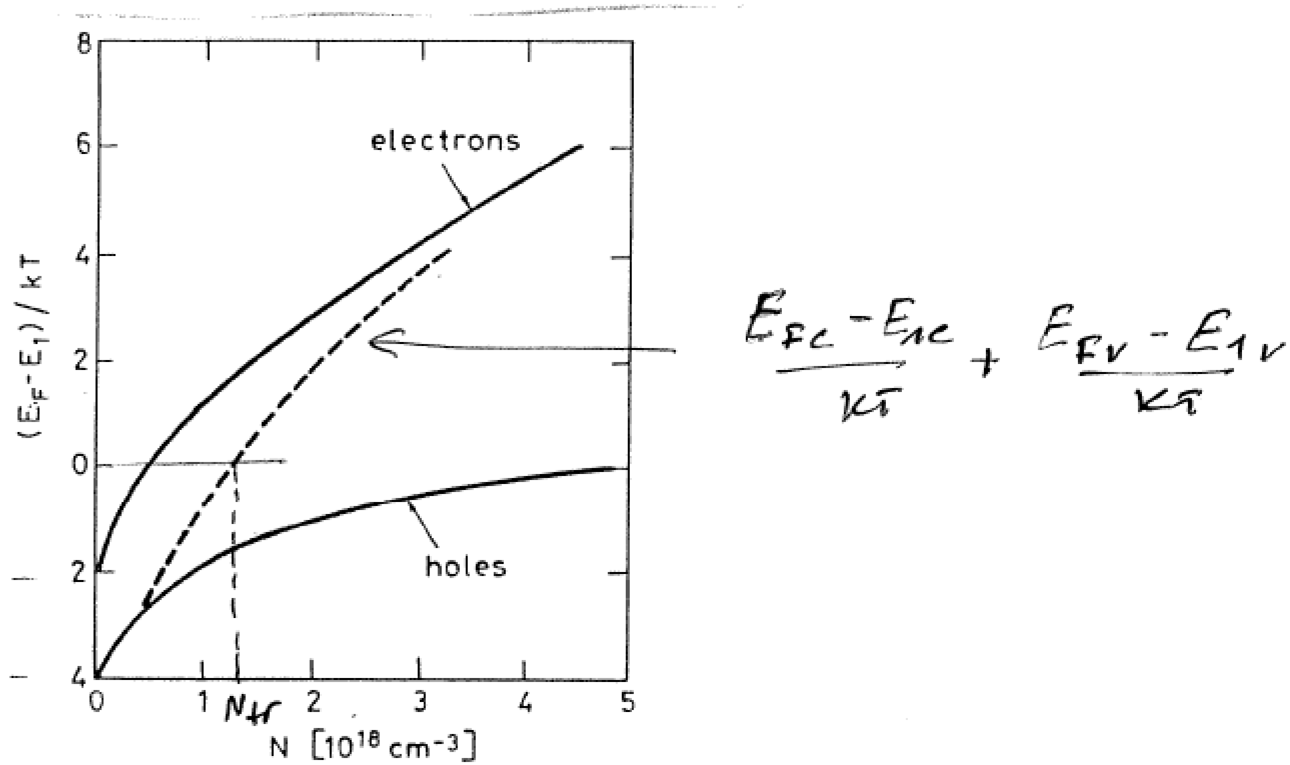

FIG. 3.26. Plots of the normalized difference between the quasi-Fermi energy E_F and the energy of the $n = 1$ subband E_1 versus density of injected carriers, for both electrons and holes, in a 10-nm GaAs/AlGaAs quantum well.

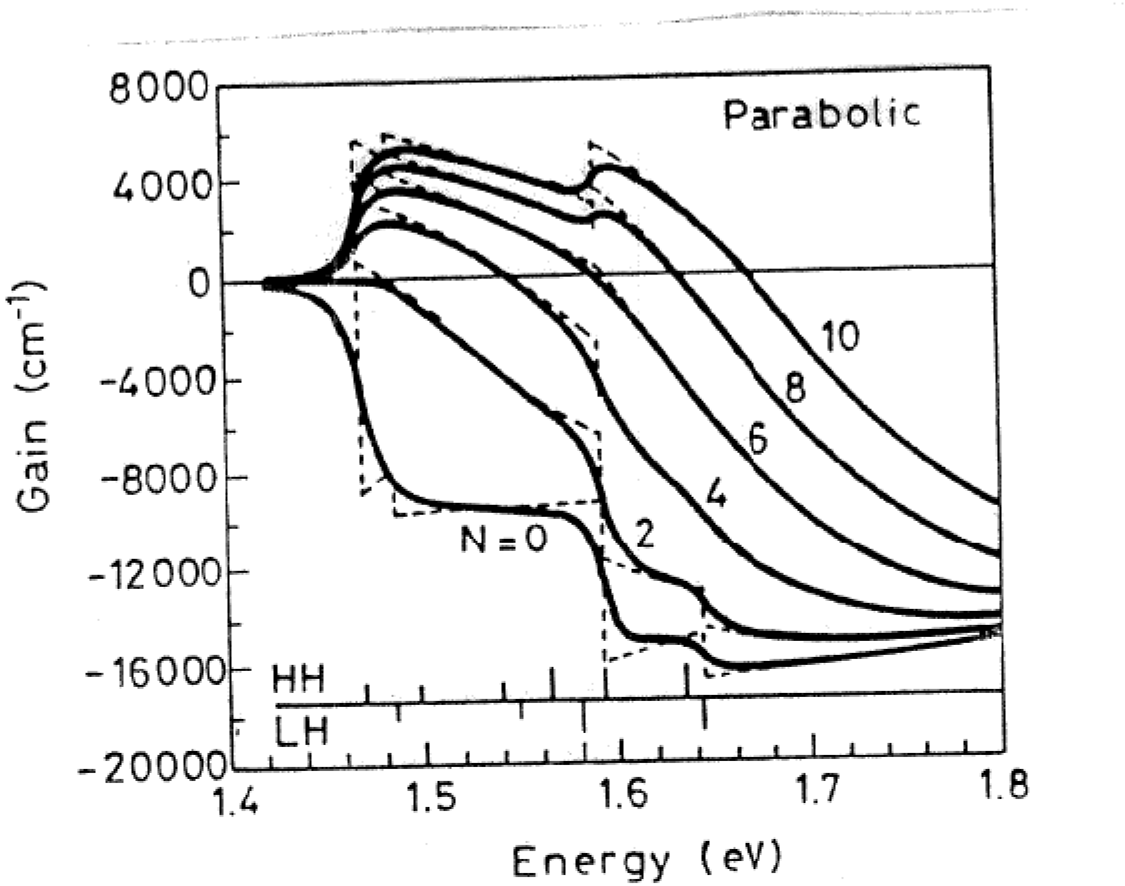

Parabolic
8000
4000
0
-4000
-8000
-12000
-16000
-20000
Gain (cm^{-1})
10
8
6
4
2
N = 0
HH
LH
1.4
1.5
1.6
1.7
1.8
Energy (eV)

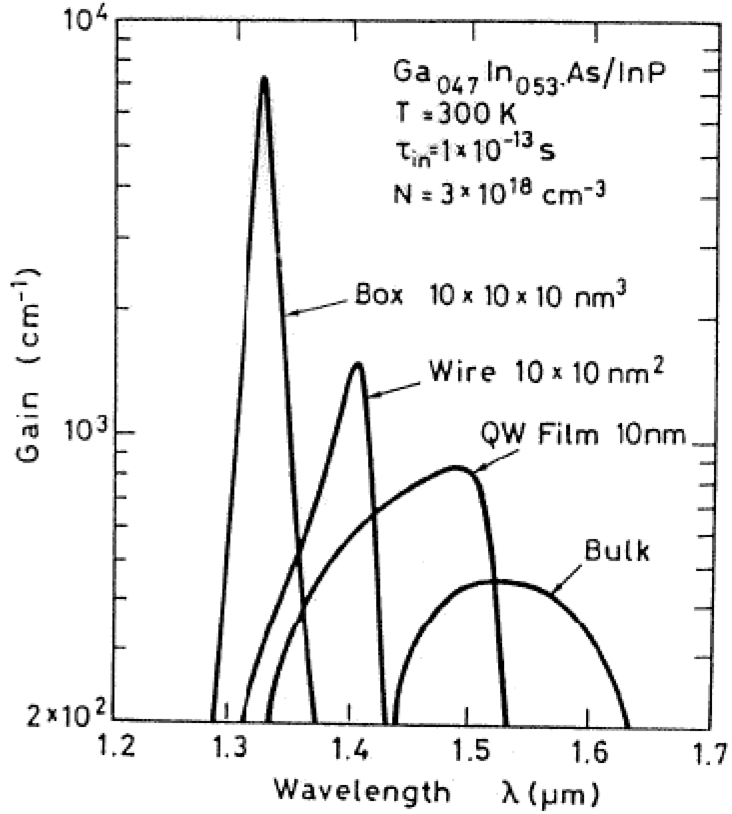

FIG. 3.31. Plot of calculated gain coefficient versus emission wavelength at $N = 3 \times 10^{18}$ cm^{-3} electron injection for a $Ga_{0.47}In_{0.53}$. As bulk semiconductor, $Ga_{0.47}In_{0.53}As/InP$ 10-nm quantum well, 10 nm × 10 nm quantum wire, and 10 nm × 10 nm × 10 nm quantum dot (box). (By permission from Ref. 19.)

Ridge lasers

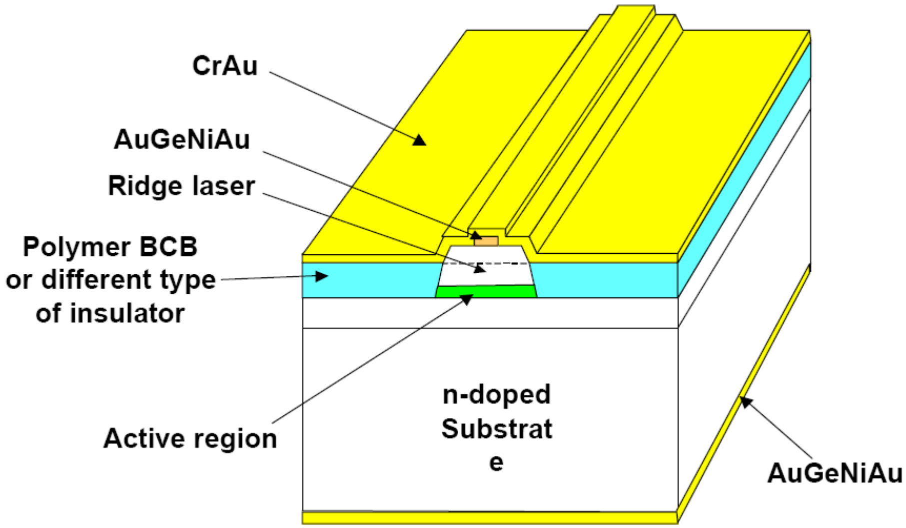

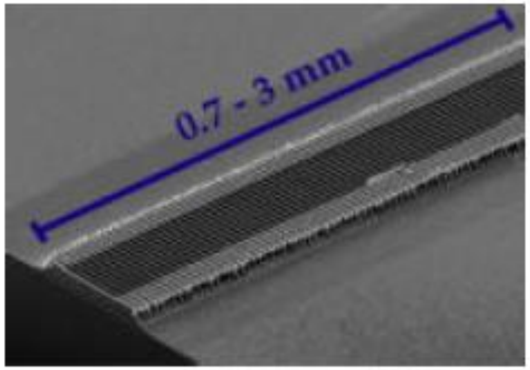

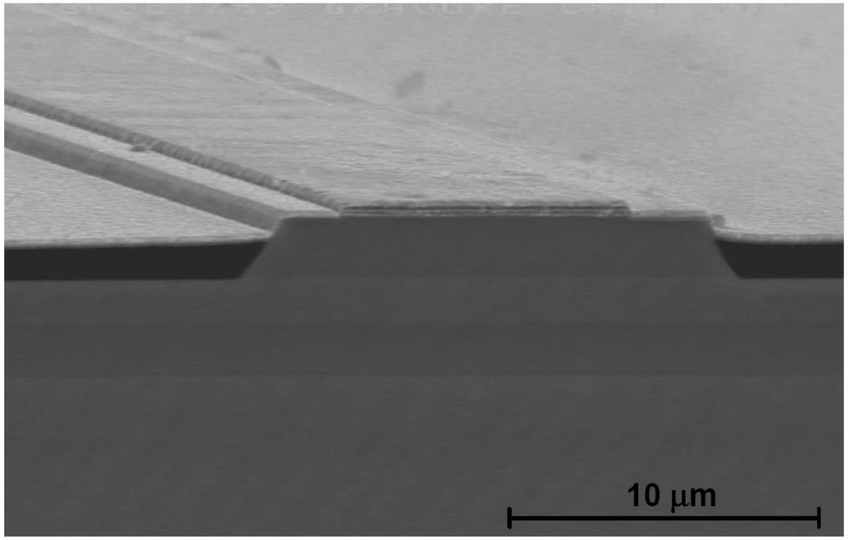

High-power semiconductor lasers

Bar of 8 BA lasers 100 µm * 2 mm, emissive length = 2.6 mm

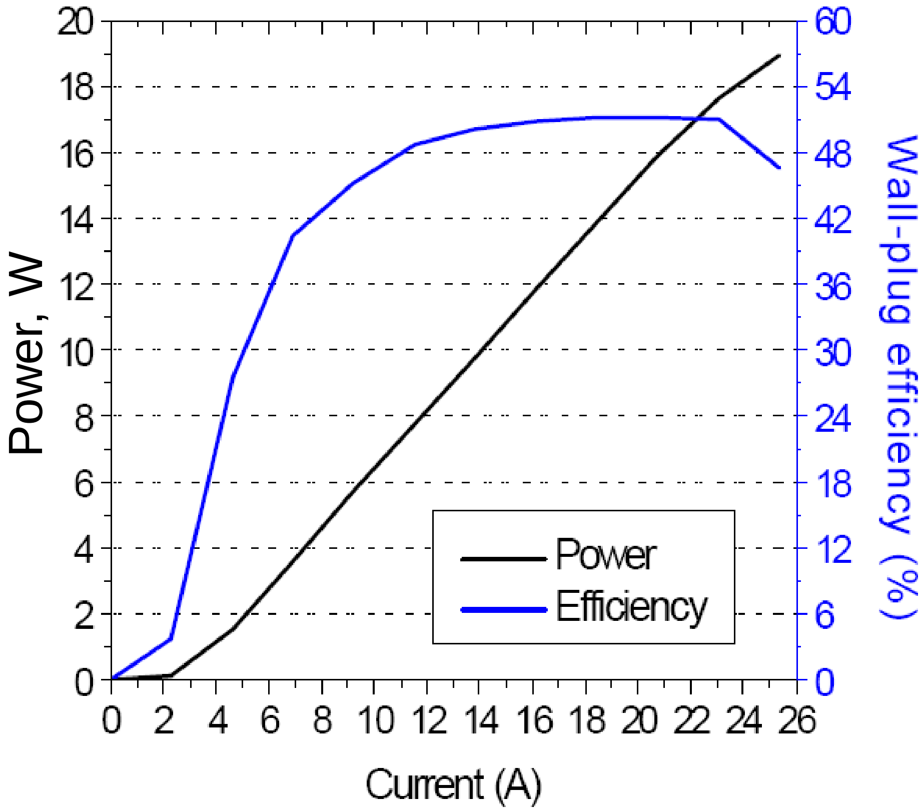

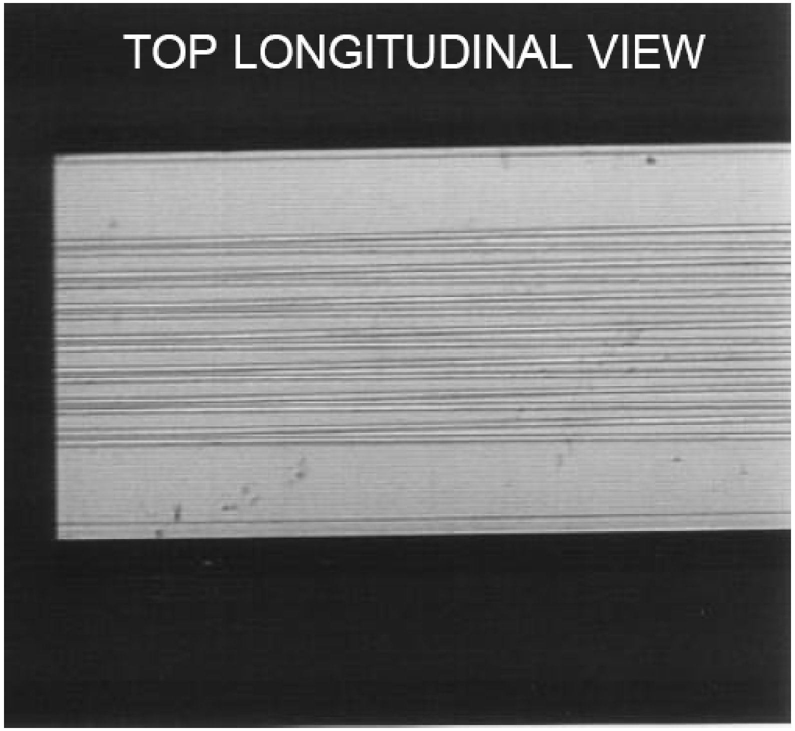

Plug Eff.= 51% on a wide range

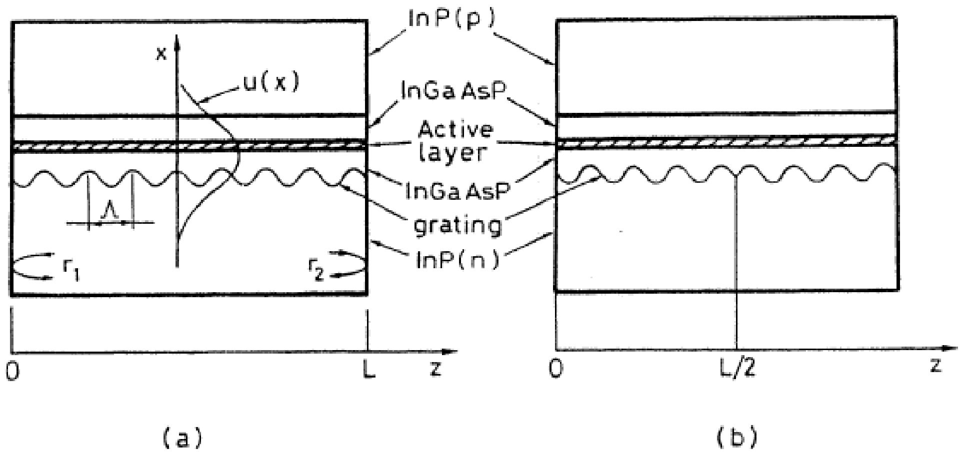

FIG. 9.29. Schematic structure of (a) DFB laser with a uniform grating and (b) $\lambda/4$-shifted DFB laser.

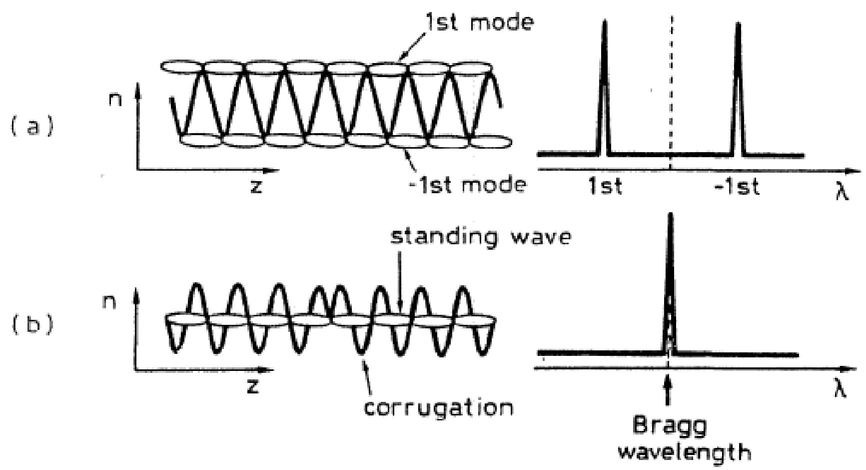

FIG. 9.31. Schematic representation of the refractive index change, mode patterns, and corresponding resonance wavelengths for a DFB laser with a uniform grating and for a DFB laser with a $\lambda/4$-shifted grating. (By permission from Ref. 49.)

VCSEL

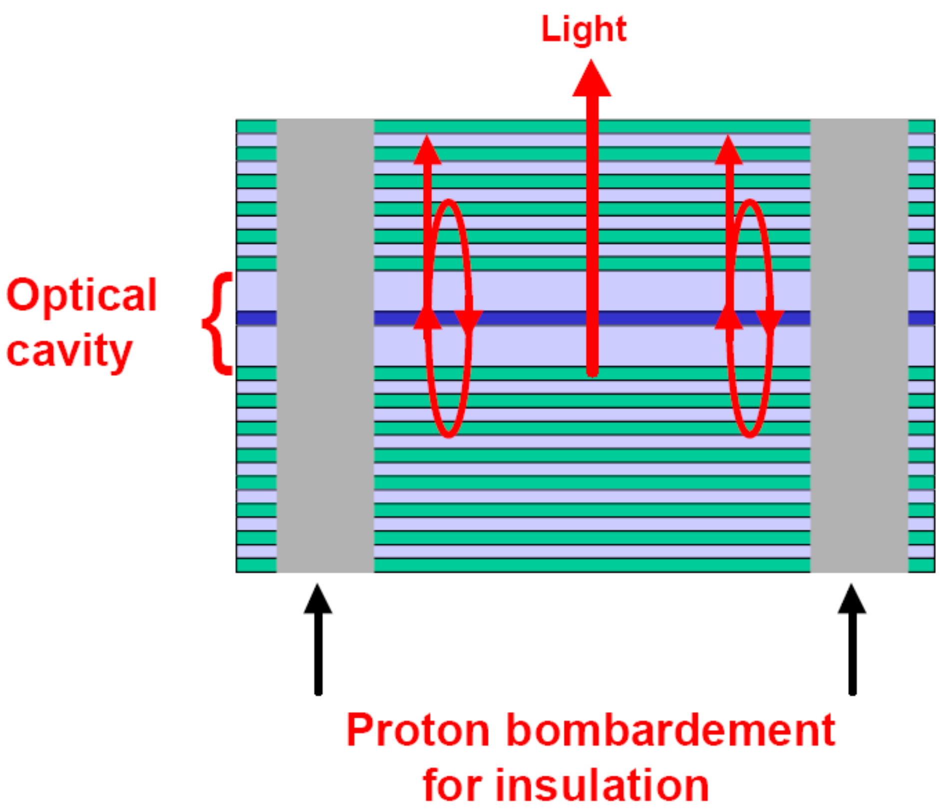
Light
Optical cavity
Proton bombardement for insulation

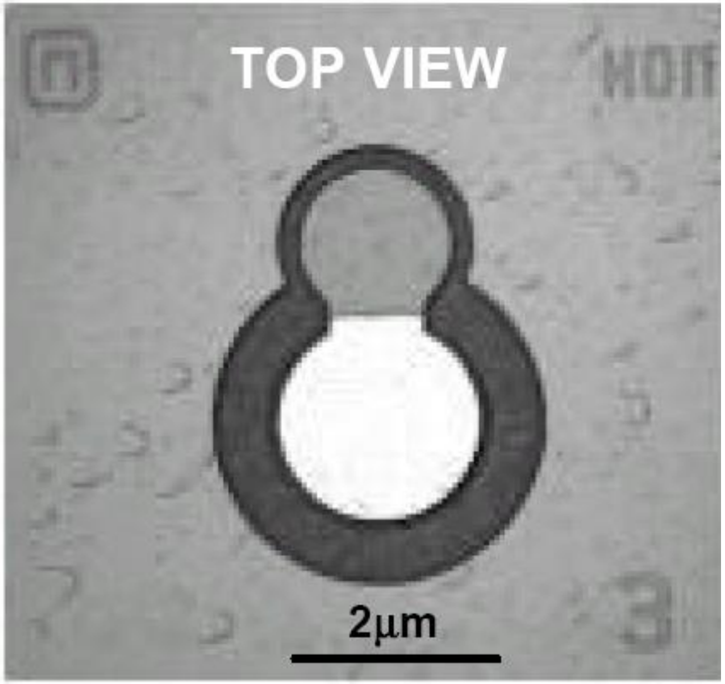
TOP VIEW
2μm

Quantum Cascade Lasers (QCL)

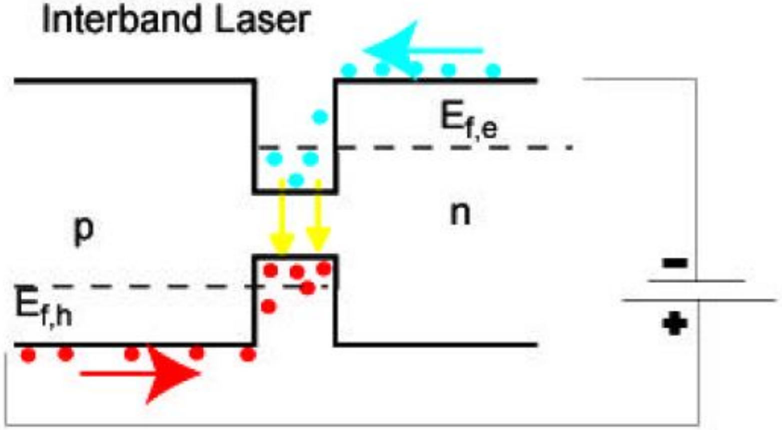

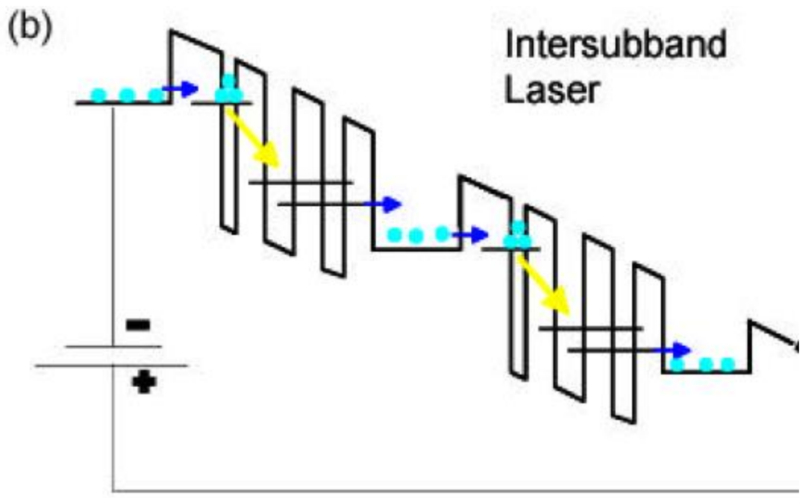

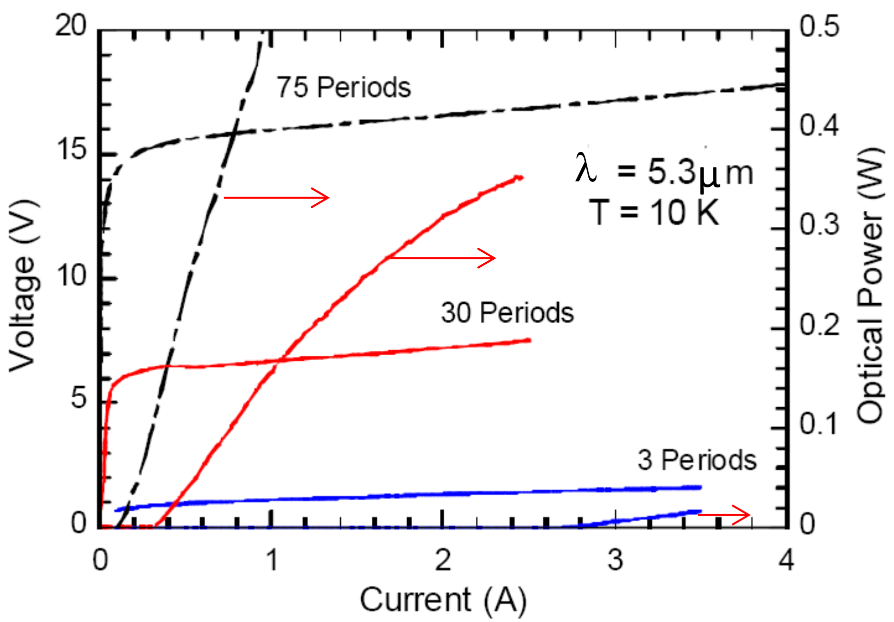

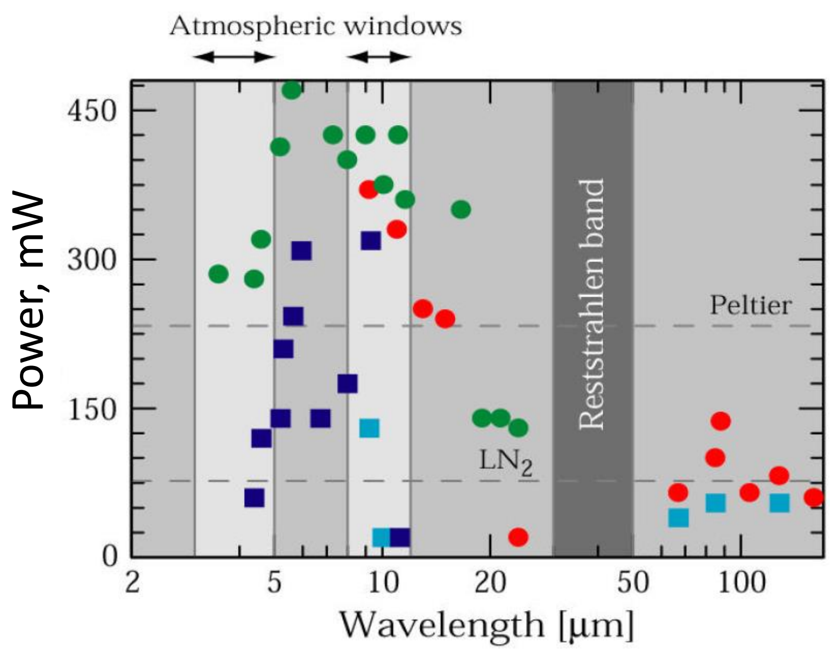

Applications of LDs

Edge emitters

- High power
- High electrical-to optical efficiency
- Relatively poor beam quality

Material processing welding,pump sources for other lasers,
Telecoms for low-power LDs

VCSELS

- Good beem quality
- Difficult to scale up power with electric pumping

Use as a gain material for optically pumped laser (OPSL)
Chip-to-chip communications, telecoms

DFB, DBR, QCL

- Narrow lainewidth
- Long wavelengths possible
- Low power

Spectroscopy, sensing, optical communications

Host dielectrics

- Al_2O_3
- Y_2O_3, Lu_2O_3, Sc_2O_3
- $YAlO_3$ (YALO, YAP)
- $Y_3Al_5O_{12}$ (YAG)
- YVO_4 (YVO), $GdVO_4$ (GVO)
- $KGd(WO_4)_2$ (KGW), $KY(WO_4)_2$ (KYW)

- $YLiF_4$ (YLF)
- $LuLiF_4$ (LuLiF)
- $LiCaAlF_6$ (LiCAF)

- Glass

Dielectric lasers

- Powers in all classes available
- CW, Q-switched, mode-locked
- From UV (190 nm) to mid-infrared
- High concentration laser media:
  - Compact lasers
  - Efficient pumping with laser diodes
- Applications: all

- Main lasing species:

Rare-earth ions:
Er^{3+}: 1.55 μm, 3μm
Nd^{3+}: 0.94 μm, 1049 nm -1079 μm
Yb^{3+}: 1 μm – 1.1 μm
Tm^{3+}: 2 μm – 2.2 μm
Ce^{3+}: 0.3 μm

Transitional metal ions (vibronic lasers):
Cr^{4+}:1.2 μm – 1.55 μm
Cr^{3+}: 0.694 μm-0.9 μm, 1.2 μm – 1.4 μm
Cr^{2+}: 2 μm – 3 μm
Ti^{3+}: 0.7 μm – 1.080 μm
Fe^{2+}: 4 μm – 5 μm

TABLE 9.1. Electronic configurations of some rare earth and transition metals of interest as laser-active impurities

Atom	Electron Configuration
Xenon, Xe[a]	(Kr)$4d^{10}5s^{2}5p^{6}$
Neodymium, Nd	(Xe)$4f^{4}5d^{0}6s^{2}$
Holmium, Ho	(Xe)$4f^{11}5d^{0}6s^{2}$
Erbium, Er	(Xe)$4f^{12}5d^{0}6s^{2}$
Thulium, Tm	(Xe)$4f^{13}5d^{0}6s^{2}$
Ytterbium, Yb	(Xe)$4f^{14}5d^{0}6s^{2}$
Chromium, Cr	(Ar)$3d^{5}4s^{1}$
Titanium, Ti	(Ar)$3d^{2}4s^{2}$
Cobalt, Co	(Ar)$3d^{7}4s^{2}$
Nickel, Ni	(Ar)$3d^{8}4s^{2}$

[a] For reference, the fundamental configuration of Xe is also shown.

Nd³⁺ active ion

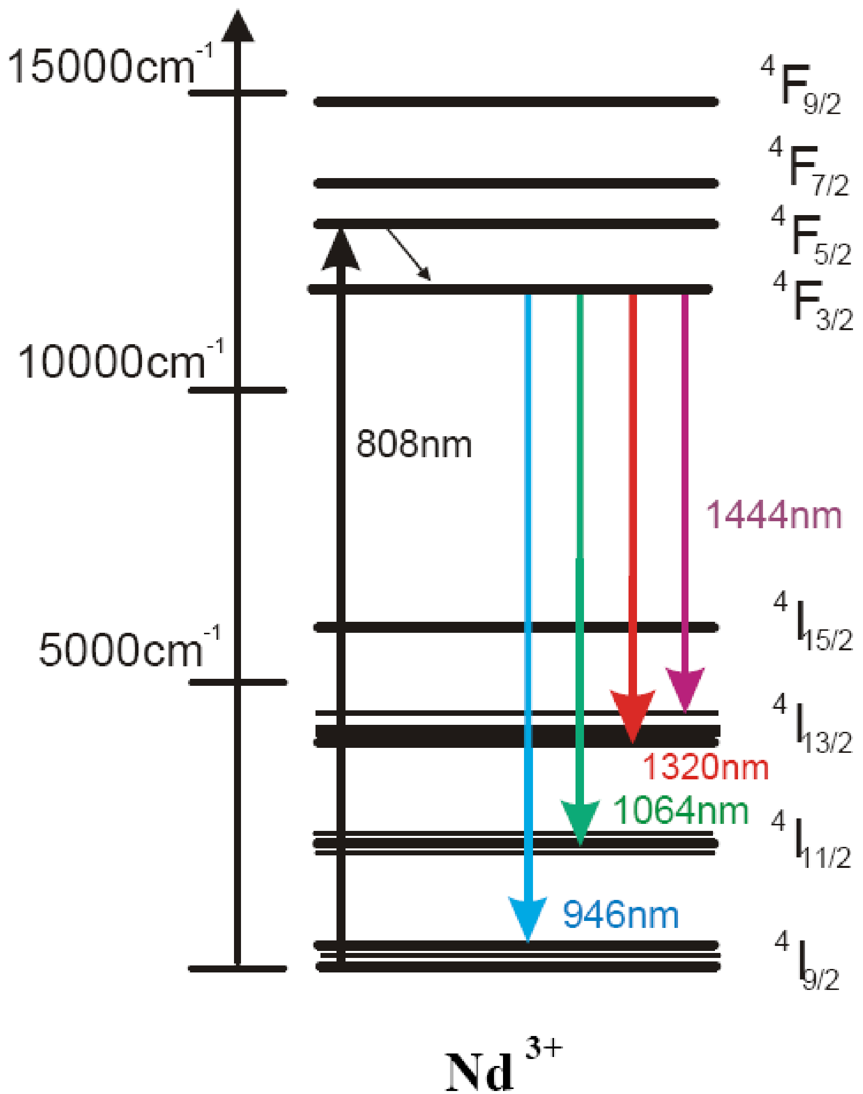

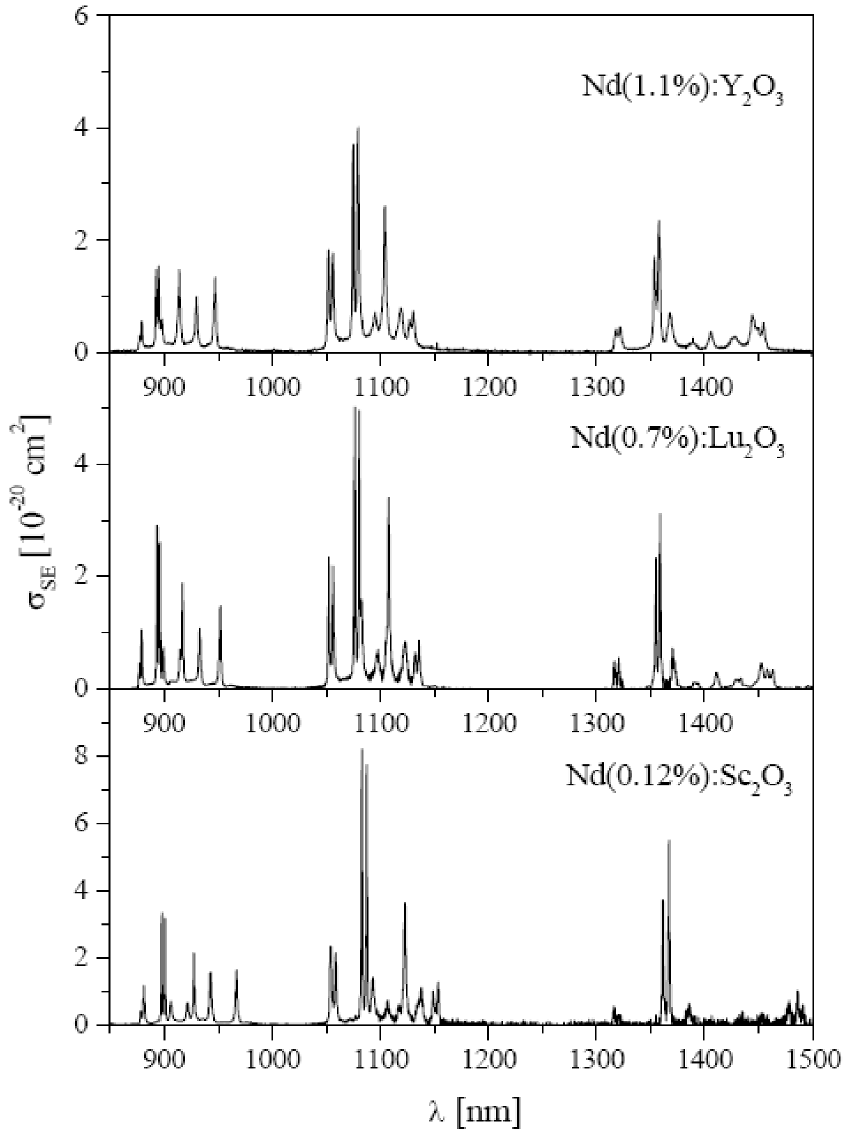

TABLE 9.3. Optical and spectroscopic parameters of Nd:YAG ($\lambda = 1.064\ \mu m$), Nd:YVO_4, Nd:YLF ($\lambda = 1.053\ \mu m$), and Nd:glass (phosphate)

	Nd:YAG $\lambda = 1.064\ \mu m$	Nd:YVO_4 $\lambda = 1.064\ \mu m$	Nd:YLF $\lambda = 1.053\ \mu m$	Nd:glass $\lambda = 1.054\ \mu m$ (Phosphate)
Nd doping	1 atom.%	1 atom.%	1 atom.%	3.8% by weight of Nd_2O_3
N_t (10^{20} ions/cm^3)[a]	1.38	1.5	1.3	3.2
τ (μs)[b]	230	98	450	300
$\Delta\nu_0$ (cm^{-1})[c]	4.5	11.3	13	180
σ_e (10^{-19} cm^2)[d]	2.8	7.6	1.9	0.4
Refractive index	$n = 1.82$	$n_o = 1.958$ $n_e = 2.168$	$n_o = 1.4481$ $n_e = 1.4704$	$n = 1.54$

[a] N_t is the concentration of the active ions, [b] τ is the fluorescence lifetime, [c] $\Delta\nu_0$ is the transition linewidth (FWHM). [d] σ_e is the effective stimulated emission cross section. Data refer to room temperature operation.

Yb^{3+} active ion

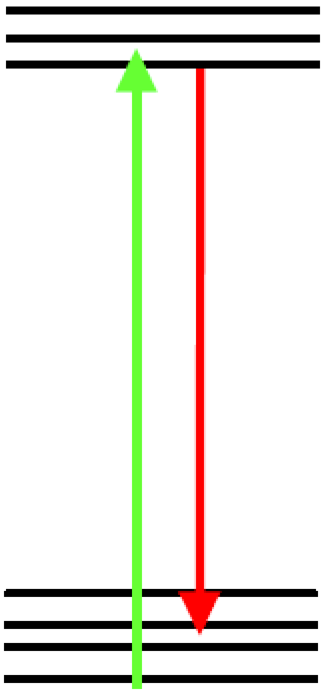

Advantages:

- Small quantum defect
- No excited state absorption (ESA)
- No up-conversion processes
- Efficient absorption of InGaAs diode light

Disadvantage:

- Boltzmann occupation of the lower laser level (quasi 4-level laser scheme)

Yb^{3+} active ion

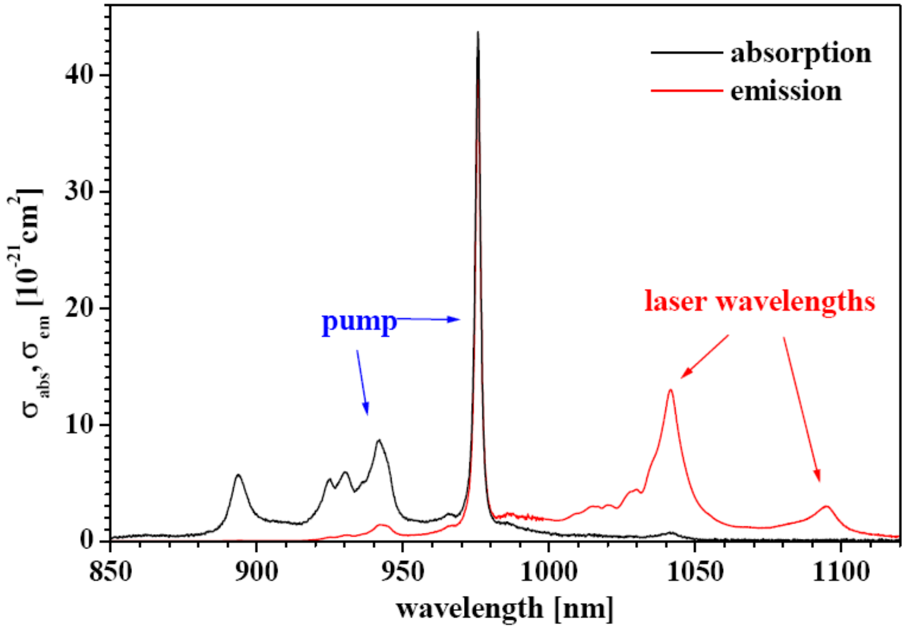

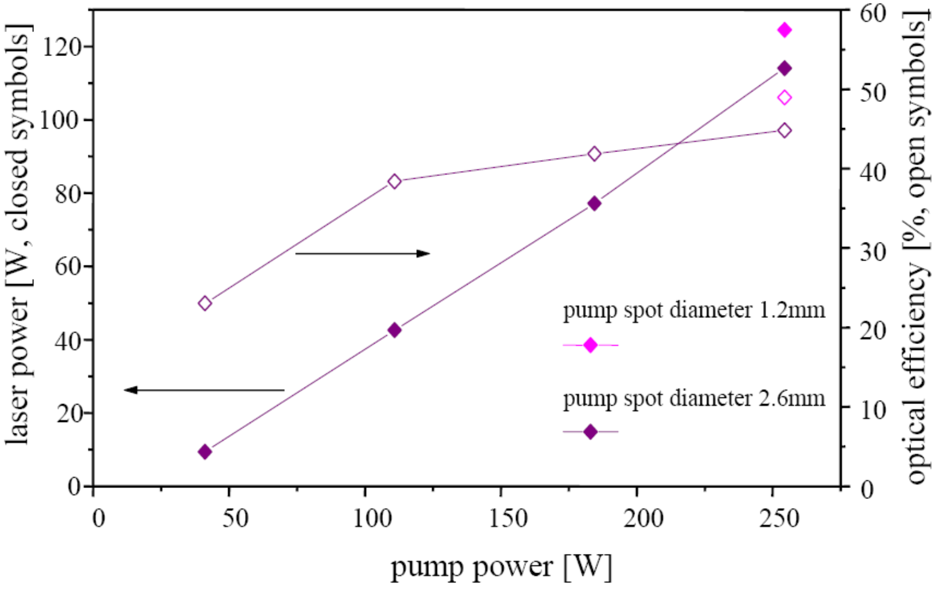

Er:Yb system: excitation transfer

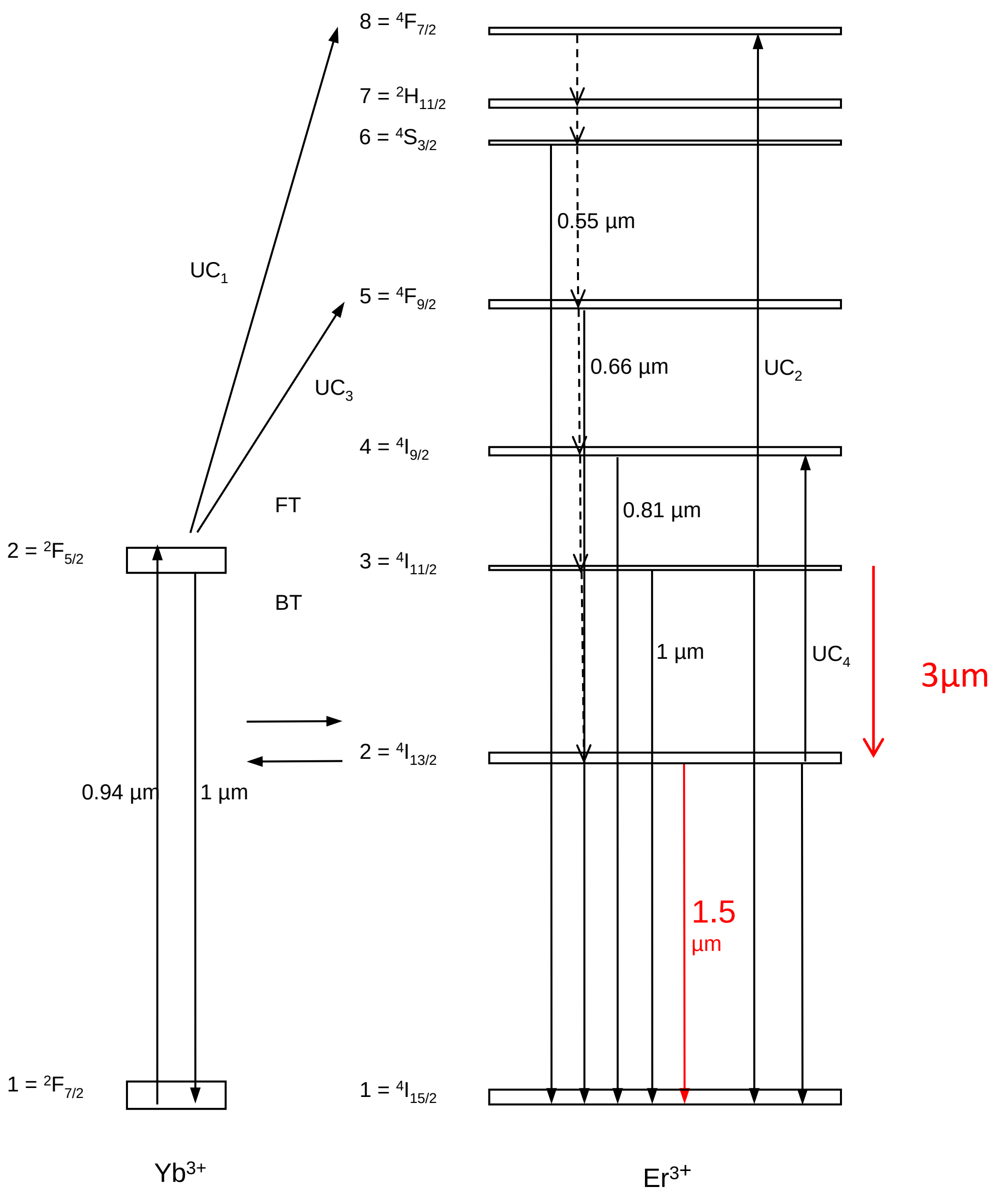

Er^{3+} : glass

Quasi-3-level system

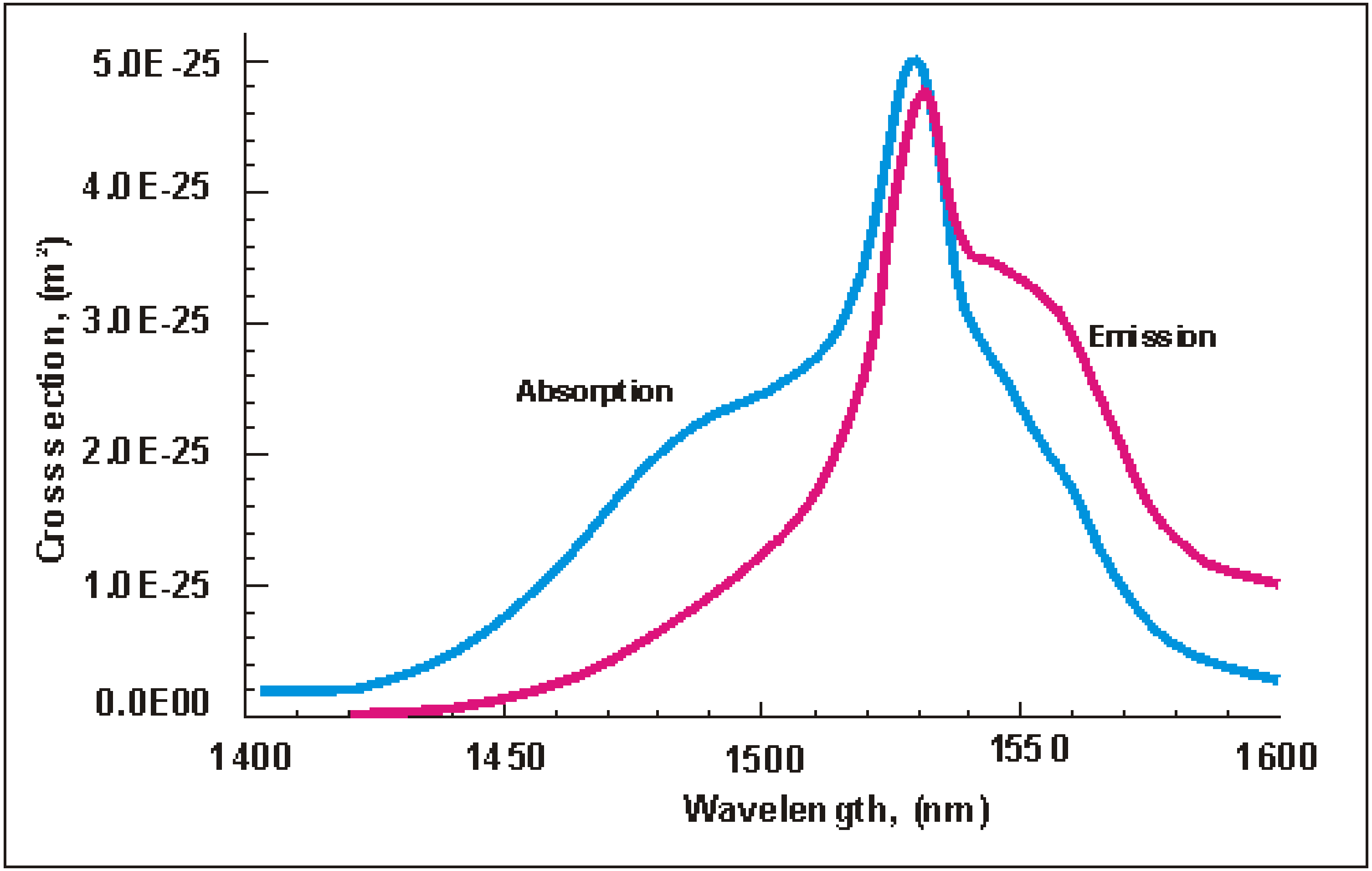

Pr^{3+} active ion

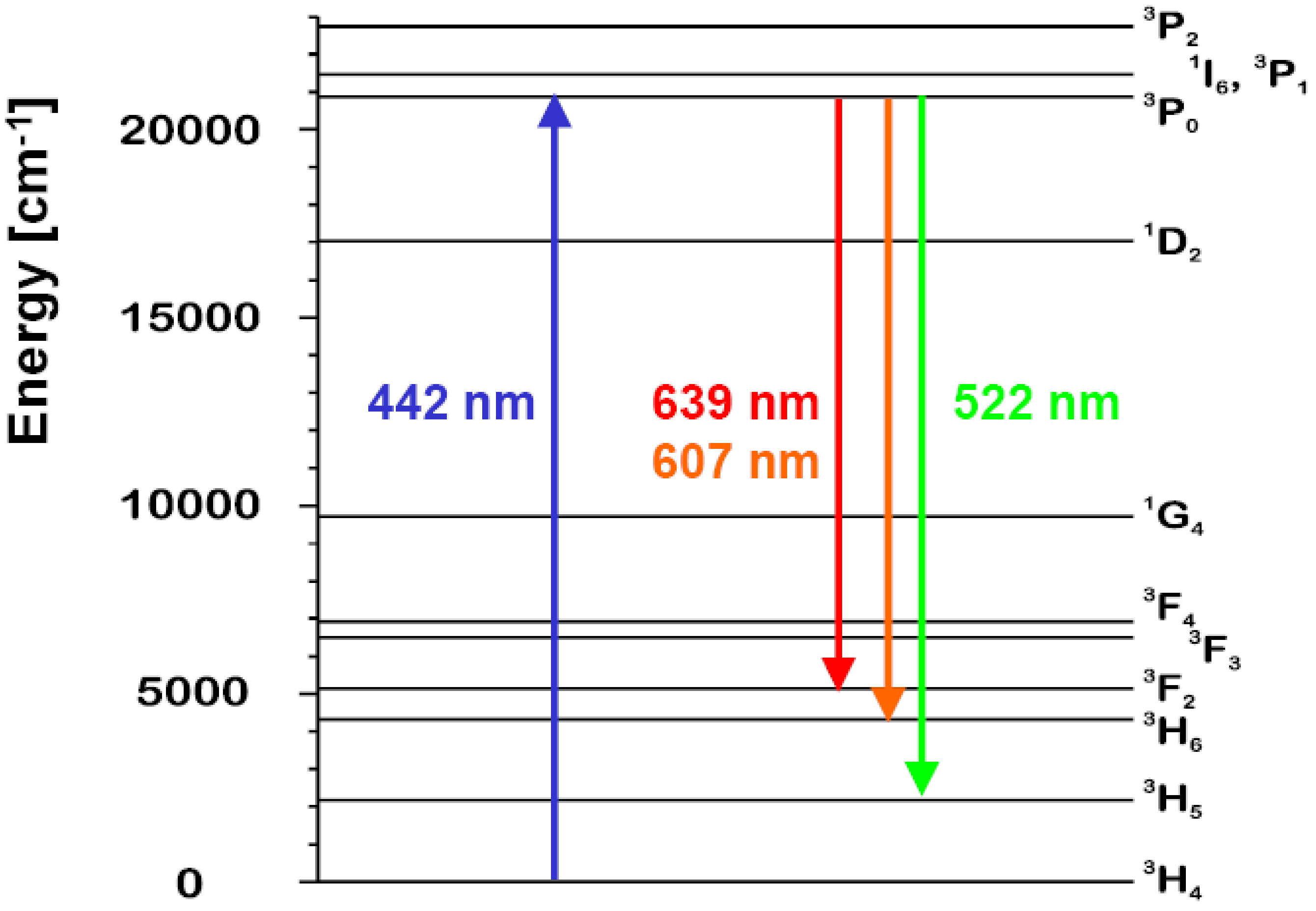

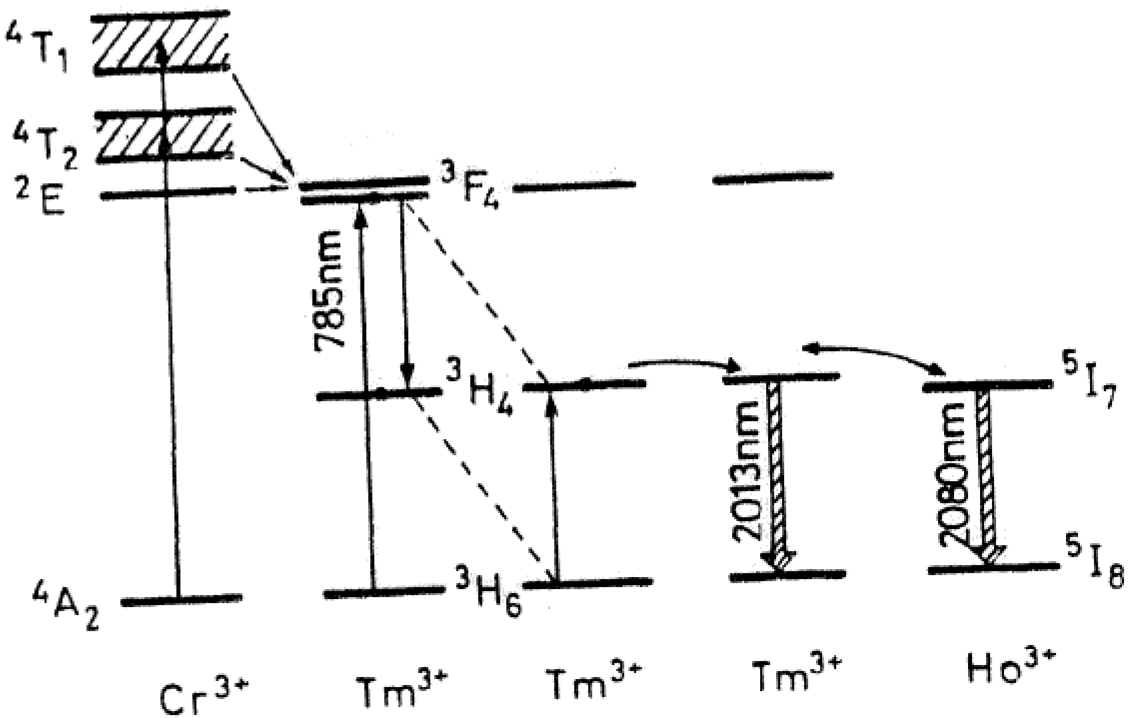

FIG. 9.5. Relevant energy level diagram of Cr:Tm:Ho:YAG system.

TABLE 9.4. Optical and spectroscopic parameters at room temperature of the most important quasi-three-level laser materials

Active Medium Parameters	Yb:YAG $\lambda = 1.03\ \mu m$	Nd:YAG $\lambda = 946\ \mu m$	Tm:Ho:YAG $\lambda = 2.091\ \mu m$	Yb:Er:Glass[a] $\lambda = 1.54\ \mu m$ (Phosphate)
Doping (atom.%)	6.5 atom.	1.1 atom.		
N_t (10^{20} ions/cm^3)	8.97	1.5	8 (Tm) 0.5 (Ho)	10 (Yb) 1 (Er)
τ (ms)	1.16	0.23	8.5	8
$\Delta\nu_0$ (cm^{-1})	86	9.5	42	120
σ_e (10^{-20} cm^2)	1.8	2.4	0.9	0.8
σ_a (10^{-20} cm^2)	0.12	0.296	0.153	0.8
Refractive index	$n = 1.82$	$n = 1.82$	$n = 1.82$	$n = 1.531$

[a] For Yb:Er:glass, the effective value of the stimulated emission and absorption cross sections are about the same, so the laser can be considered to operate in (almost) a pure three-level scheme.

Upconversion lasers

Example: Er^{3+}(1%):$LiYF_4$ ($\lambda_1=\lambda_2$)

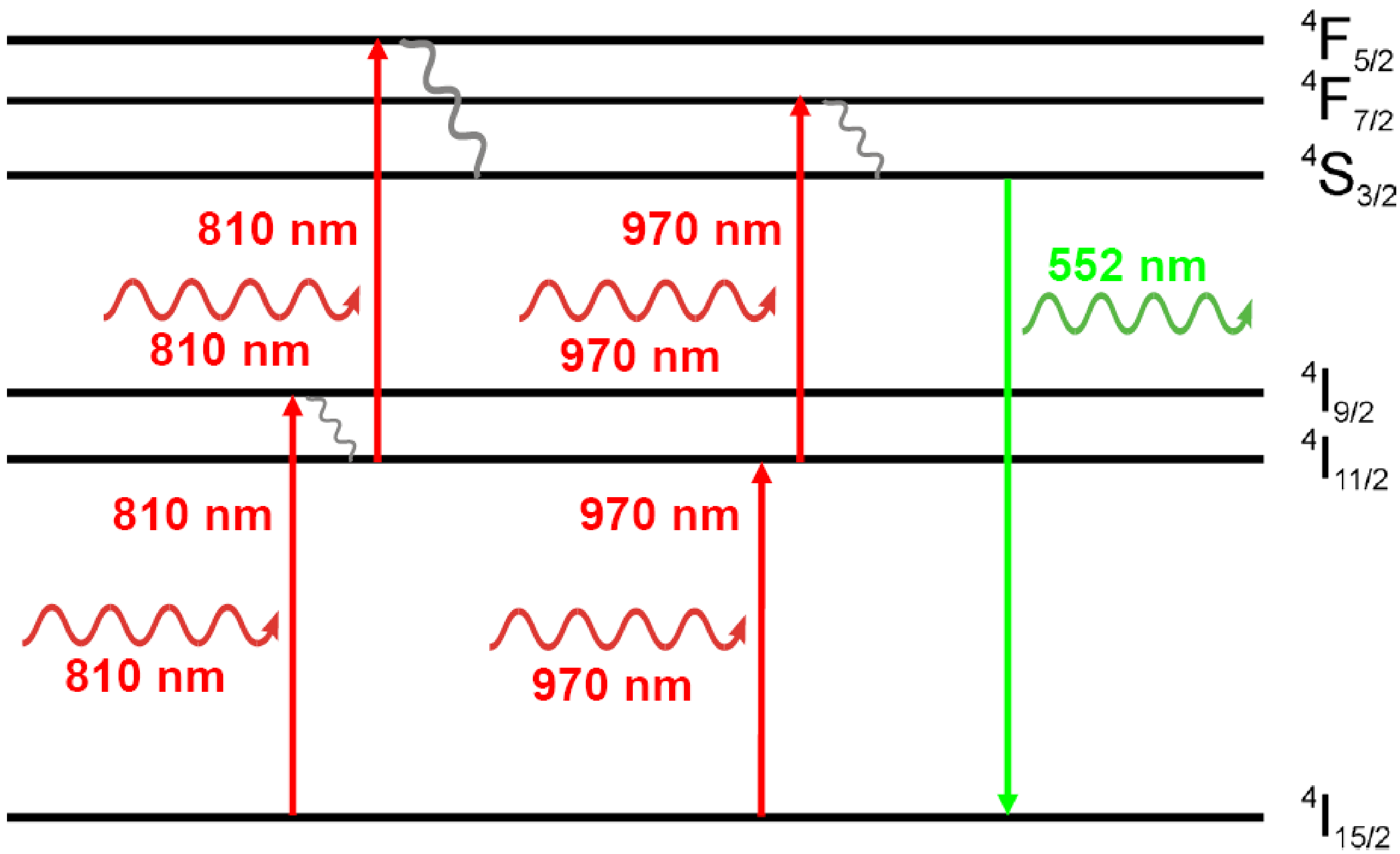

Use Low-phonon-energy hosts, e.g., ZBLAN: **Z**rF_4-**B**aF_2-**L**aF_3-**A**lF_3-**N**aF.

Optical Fibers, intro

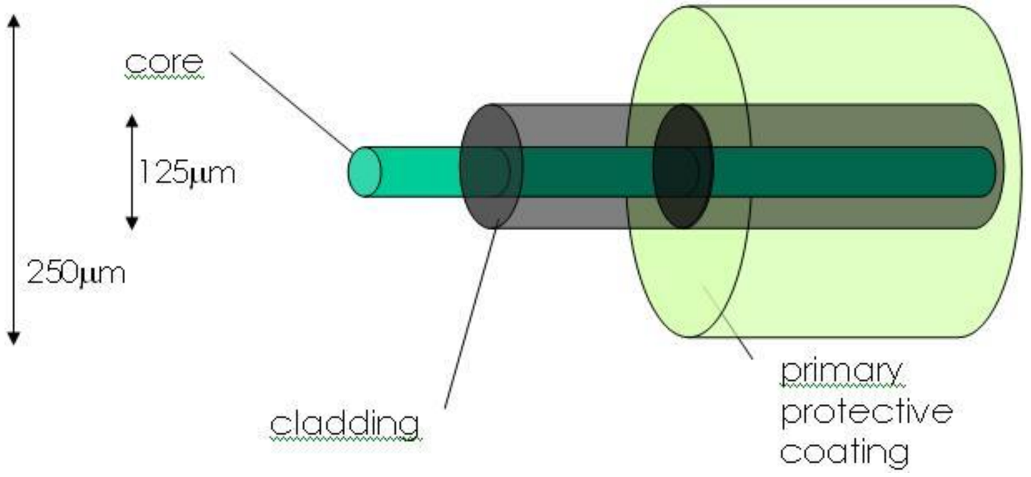

From Computer Desktop Encyclopedia

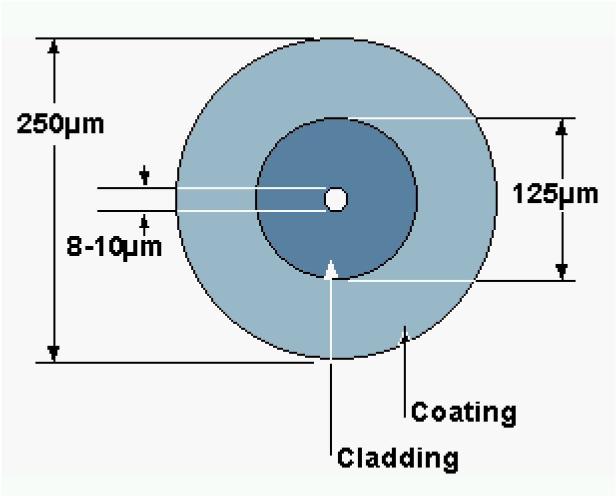

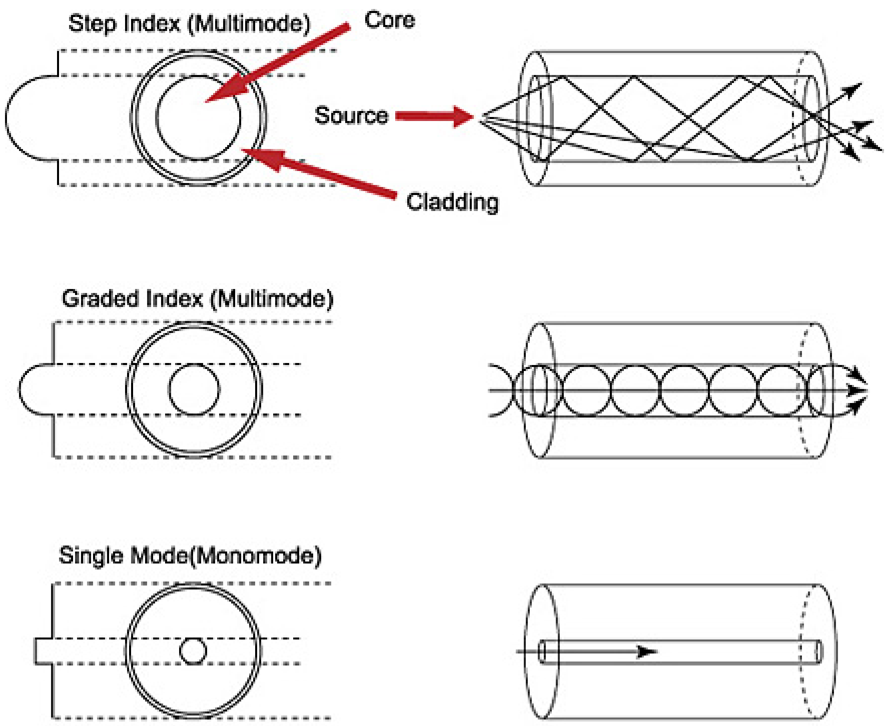

A Graphic Representation of How Light Rays Travel in Three Fiber Types

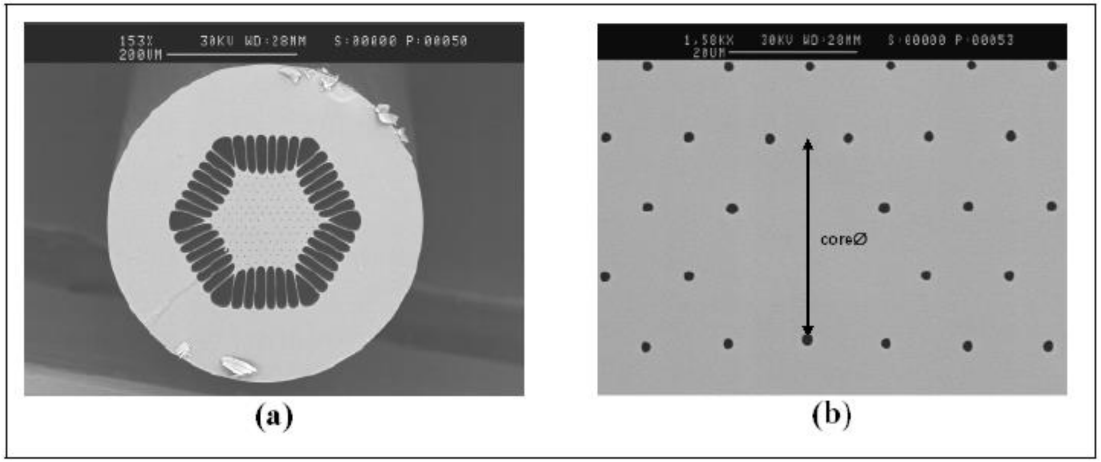
core∅
(a)
(b)

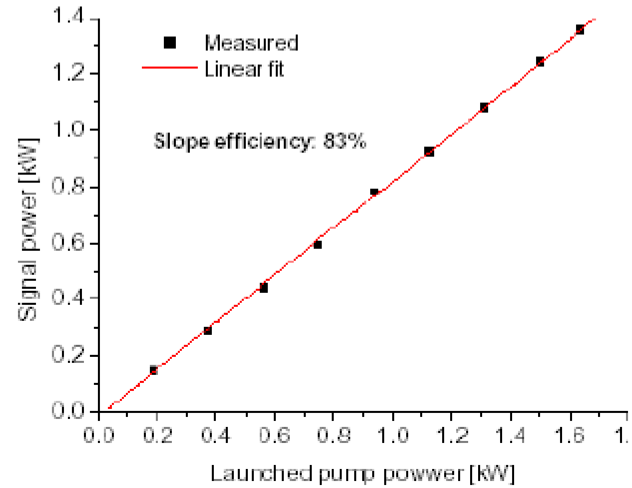
Measured
Linear fit
Slope efficiency: 83%
Signal power [kW]
Launched pump powwer [kW]
0.0
0.2
0.4
0.6
0.8
1.0
1.2
1.4
1.6
1.8

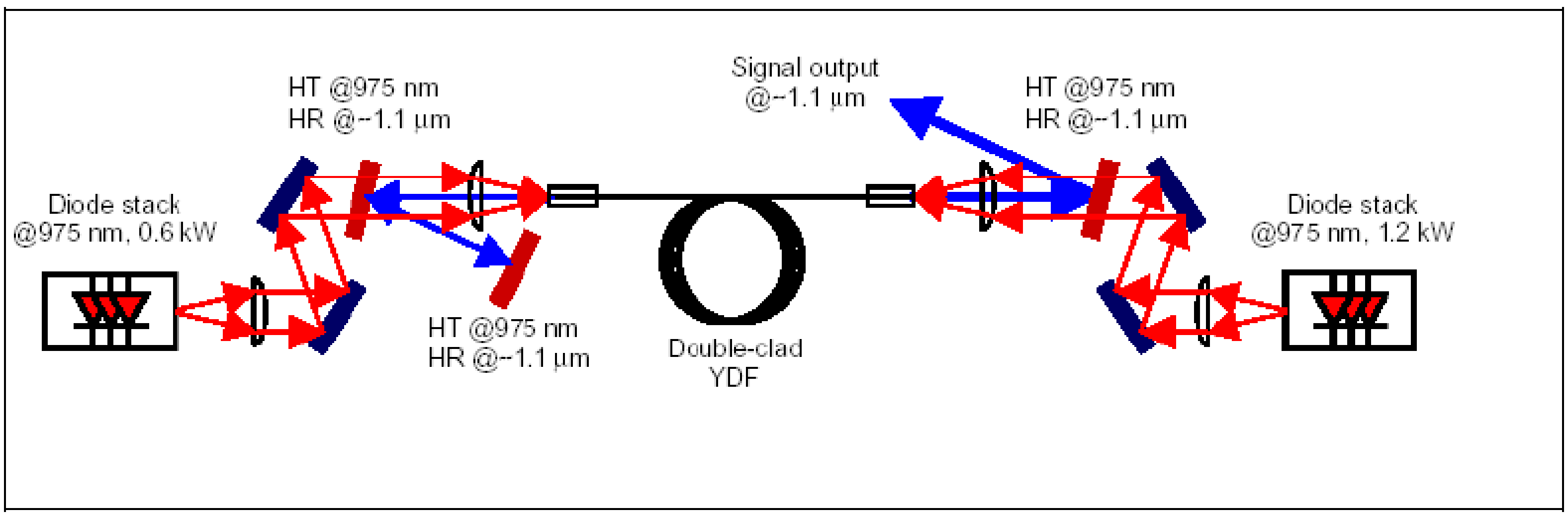
Signal output
@~1.1 μm
HT @975 nm
HR @~1.1 μm
HT @975 nm
HR @~1.1 μm
Diode stack
@975 nm, 0.6 kW
Diode stack
@975 nm, 1.2 kW
HT @975 nm
HR @~1.1 μm
Double-clad
YDF

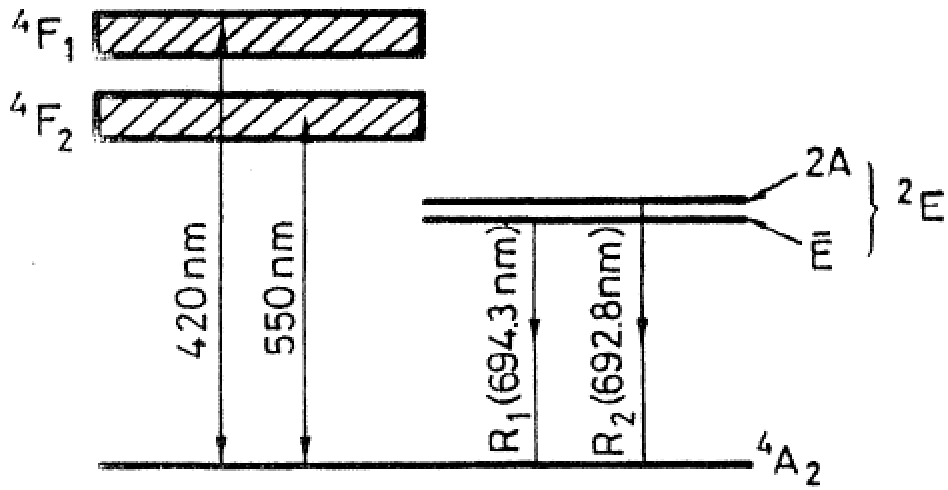

FIG. 9.1. Simplified energy levels of ruby.

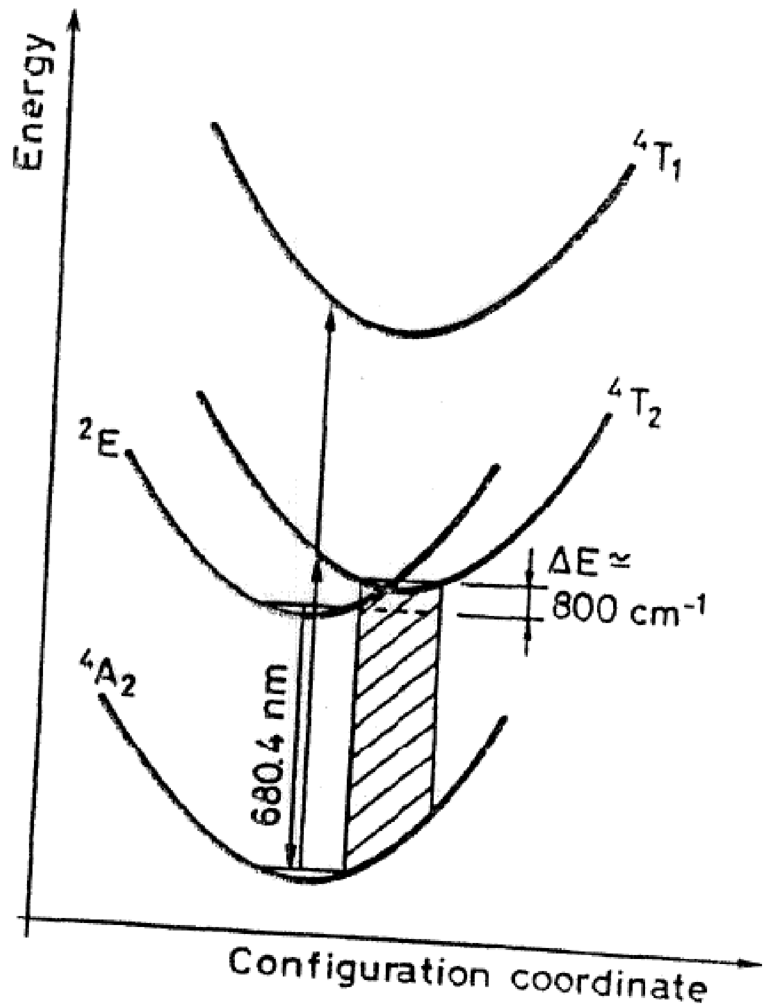

FIG. 9.8. Energy level diagram of alexandrite laser in a configuration coordinate model.

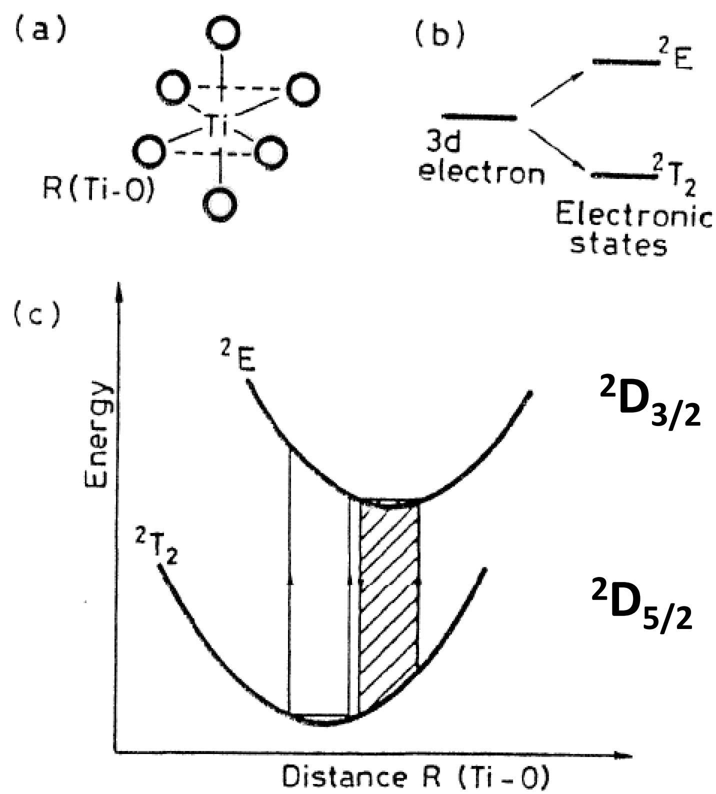

FIG. 9.9. (a) Octahedral configuration of Ti:Al_2O_3, (b) splitting of 3*d* energy states in an octahedral crystal field, and (c) energy states in a configuration coordinate model.

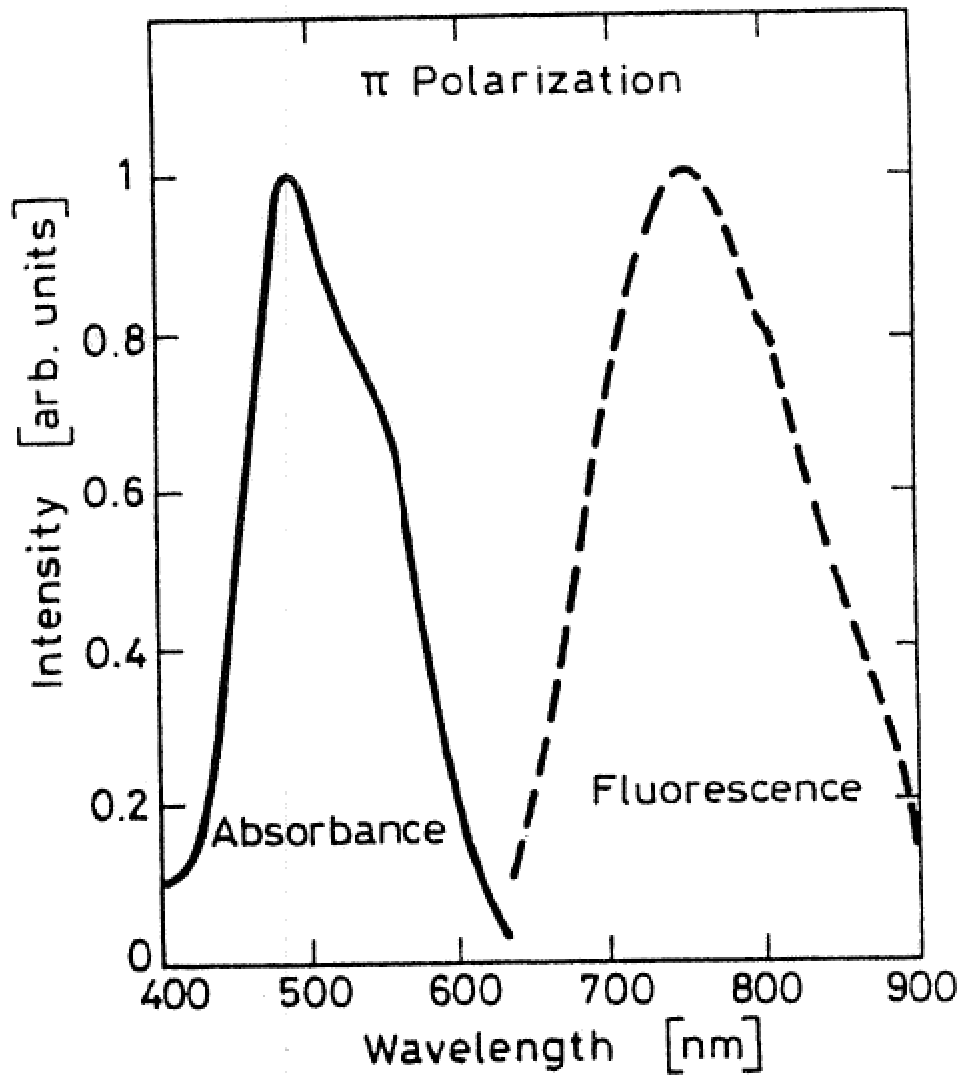

FIG. 9.10. Absorption and fluorescence bands of Ti:sapphire. (By permission from Ref. 55.)

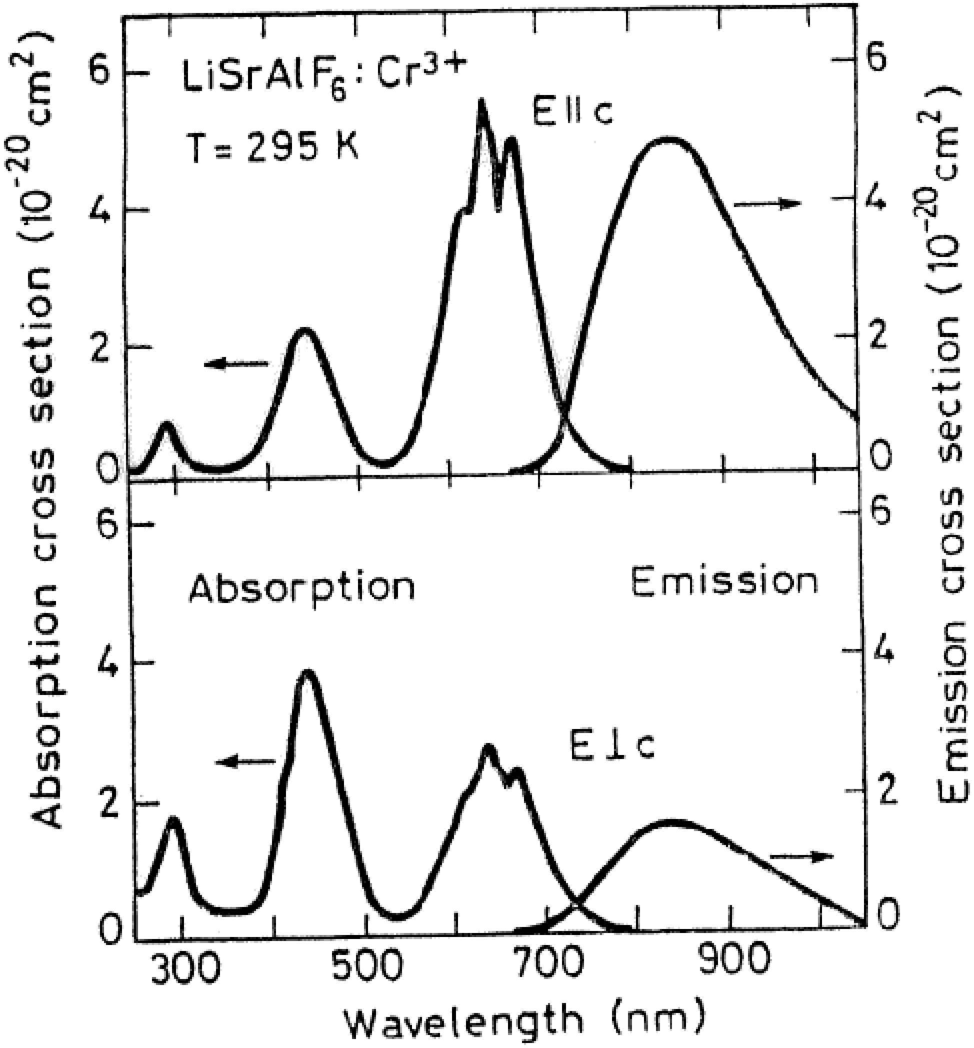

FIG. 9.11. Absorption and fluorescence bands of Cr:LiSAF for polarization parallel and perpend *c*-axis of the crystal. (By permission from Ref. 24.)

TABLE 9.5. Optical and spectroscopic parameters at room temperature of the most important tunable solid-state laser materials

Active Medium Parameters	Alexandrite	Ti:sapphire	Cr:LiSAF	Cr:LiCAF
Doping (at.%)	0.04–0.12	0.1	up to 15	up to 15
N_t (10^{19} ions/cm^3)[a]	1.8–5.4	3.3	10	10
Peak wavelength (nm)	760	790	850	780
Tuning range (nm)	700–820	660–1180	780–1010	720–840
σ_e (10^{-20} cm^2)	0.8	28	4.8	1.3
τ (μs)	260	3.2	67	170
$\Delta\nu_0$ (THz)	53	100	83	64
Refractive indices	$n_a = 1.7367$ $n_b = 1.7421$ $n_c = 1.7346$	$n_o = 1.763$ $n_e = 1.755$	$n_e = 1.4$	$n_e = 1.39$

[a] The density of active ions N_t for both Cr:LiSAF and Cr:LiCAF is given at ~1% molar concentration of CrF_3 in the melt.

Some transitional metal lasers

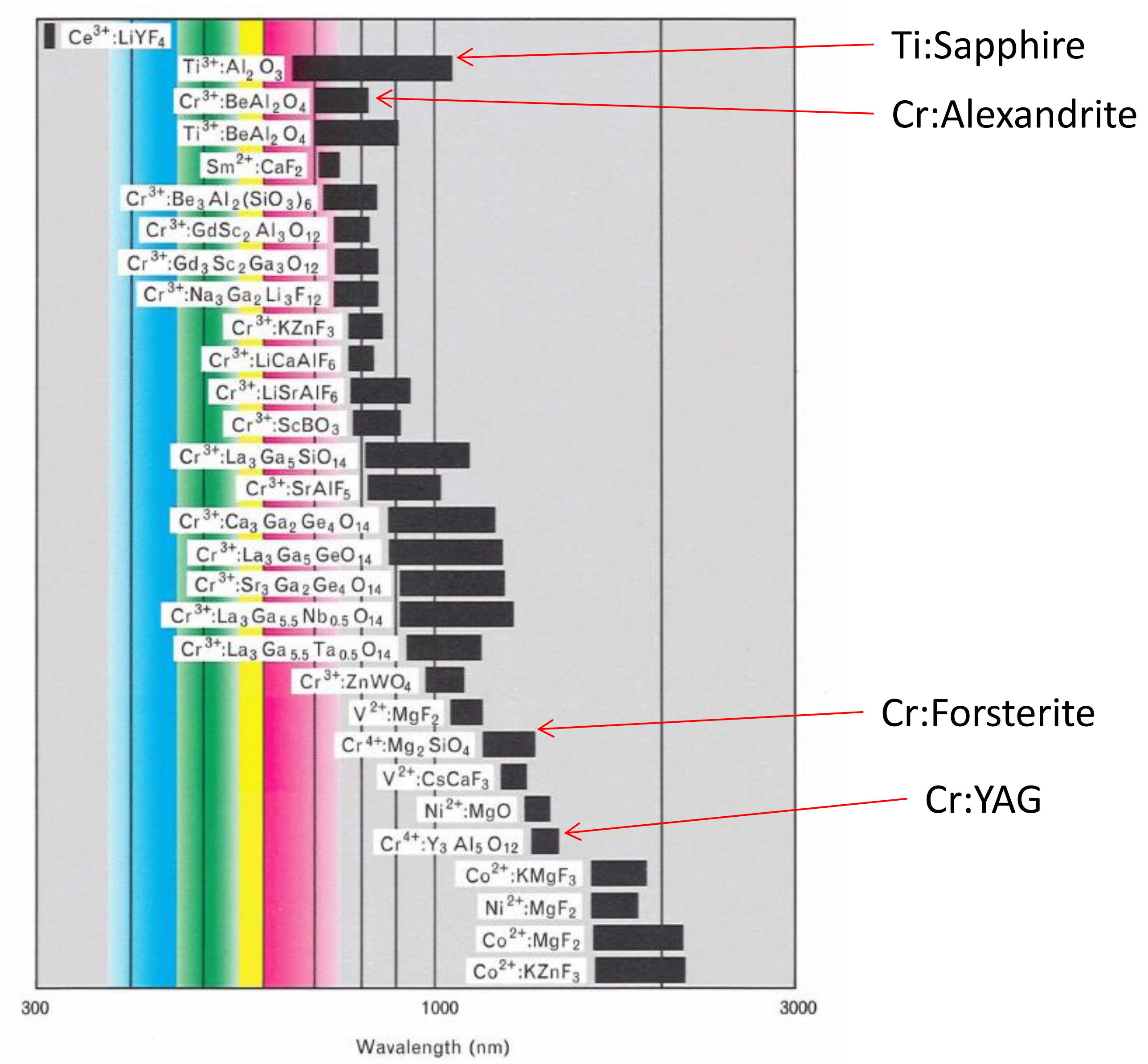

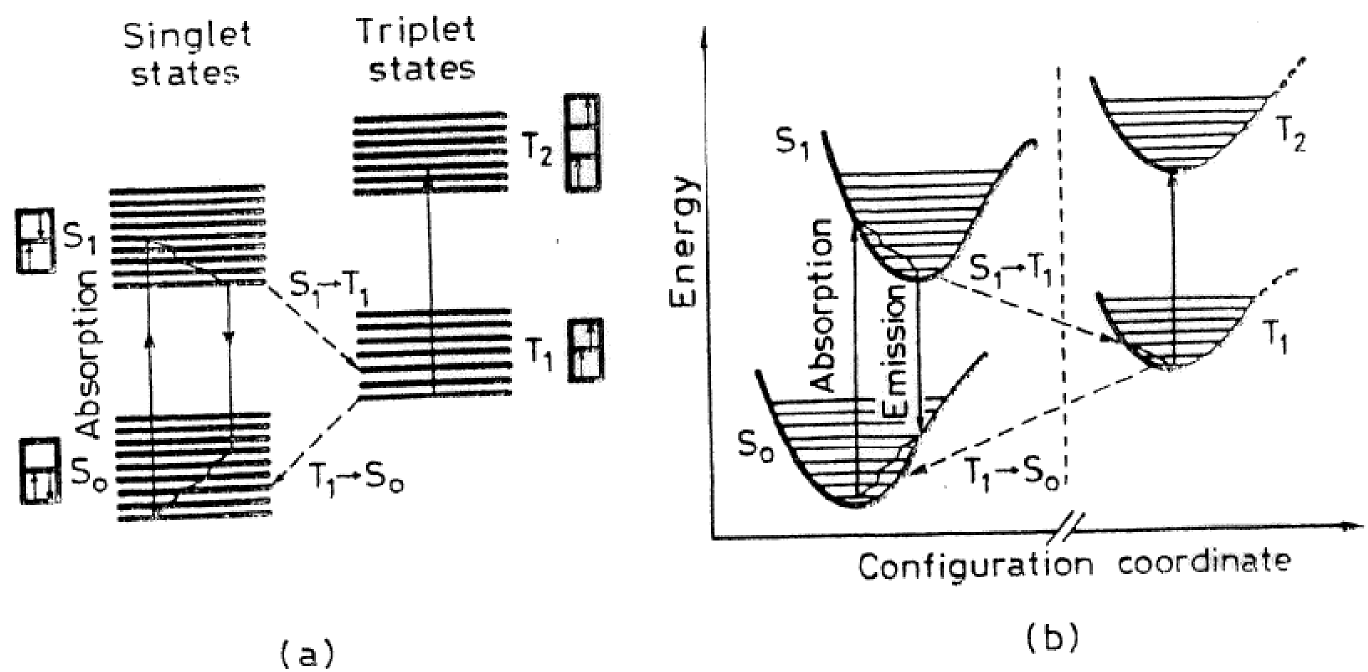

FIG. 9.15. (a) Typical energy levels for a dye in solution. The singlet and triplet states are shown in separate columns. (b) Energy level diagram of a dye in a configuration coordinate representation. (By permission from Ref. 28 with data taken from Ref. 57.)

Dye lasers

Dye	Structure	Solvent	Wavelength
Acridine red	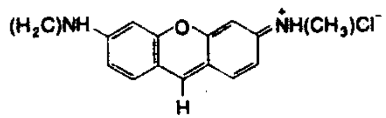	EtOH	Red 600 - 630 nm
Rhodamine 6G	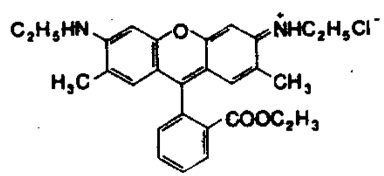	EtOH MeOH H_2O DMSO Polymethyl- methacrylate	Yellow 570 - 610 nm
Rhodamine B	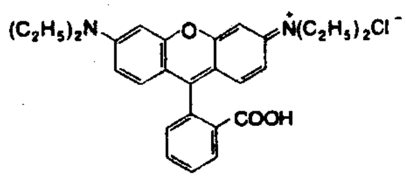	EtOH MeOH Polymethyl- methacrylate	Red 605 - 635 nm
Na-fluorescein	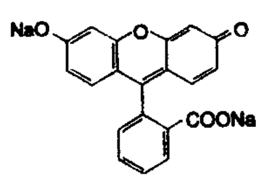	EtOH H_2O	Green 530 - 560 nm
7-Hydroxycoumarin	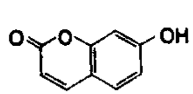	H_2O (pH~9)	Blue 450 - 470 nm

Figure 5-11 Molecular structure of several laser dyes, along with the laser wavelength range for each dye

Keywords

Rare-earth doped dielectric lasers
Transitional metal doped lasers
Vibronic lasers
Dye lasers
Double-heterojunction lasers
Separate confinement double heterjunction multiple quantum well lasers
GRINSCH lasers
VSCEL
DFB, DBR lasers, distributed feedback
Quantum cascade lasers
Large mode-area fiber lasers